

NPo-forskning fra Miljøstyrelsen

Nr. B13 1990

Flow and Transport Modelling – Rabis Field Site



Miljøministeriet **Miljøstyrelsen**

Danish Research Programme on Nitrogen, Phosphorus and Organic Matter (NPO)

The aim of the NPO Research Programme is to gather knowledge on the decomposition of Nitrogen (N), Phosphorus (P) and organic matter (o) in the soil, and on their impact on lakes, watercourses, inlets, ground-water and the sea.

This report is one of a total of about 50 reports to be issued in connection with the implementation of the NPO Research Programme. The National Agency of Environmental Protection (NAEP) is responsible for the programme, under which about 70 NPO projects have been launched, carried out at 25-30 institutions.

In the 1970's and the beginning of the 1980's there was a growing awareness of the threats to life in watercourses etc. presented by discharges of nutrients – and of the risk of nitrate contamination of groundwater. In 1984 a report was prepared, synthesising existing knowledge in this field. The report, known by the name of NPO Report, was published by the NAEP.

To follow up this report the Danish Parliament took the first steps in 1985 to reduce pollution with nutrients – laying down requirements for storage and application of farm yard manure in the agricultural sector.

For the purpose of improving our knowledge on the impact of nutrients in nature, the Danish Parliament also reserved 50 million DKK for the research programme, running from 1985 to the end of 1990.

The significance of the NPO Research Programme was further underlined with the Danish Parliament's adoption of the Action Plan on the Aquatic Environment in 1987. The results of the NPO Research Programme will play a vital role in the evaluation of the effects of the Action Plan.

To safeguard the technical and economic interests relating to the research activities a steering group was set up, having the overall responsibility for the implementation of the NPO Research Programme. Furthermore, three coordination groups were formed, each of them responsible for one of the three fields: soil and air, groundwater, and surface water.

The reports are published in the series »NPo-forskning fra Miljøstyrelsen« (NPO Research in the NAEP), divided into three sections:

A: reports on soil and air

B: reports on groundwater

C: reports on watercourses, lakes and marine waters.

The NAEP has been secretariat for the research programme. The reports published in this series are edited by the Agency with the assistance of the coordination groups.

4213

**NPo-forskning fra Miljøstyrelsen
Nr. B13 1990**

Flow and Transport Modelling – Rabis Field Site

Peter Engesgaard and
Karsten Høgh Jensen
Technical University of Denmark

**MILJØSTYRELSEN
BIBLIOTEKET
Strandgade 29
1401 København K**

**Miljøministeriet
Miljøstyrelsen**

Contents

<u>1. Summary</u>	4
<u>2. Danish summary</u>	6
<u>3. Introduction</u>	8
<u>4. Methodology</u>	10
4.1 Background	11
4.1.1 Hydrogeology	11
4.1.2 Hydrogeochemistry	13
4.2 Modelling approach	15
4.3 Modelling tools	21
2.3.1 Flow models	21
2.3.2 Tritium transport models	23
2.3.3 Reactive nitrate transport models	25
<u>5. Results</u>	28
5.1 Flow	28
5.2 Tritium transport	33
5.3 Reactive nitrate transport	42
5.3.1 Rates of redox front movement	43
5.3.2 Aquifer nitrate contamination	49
<u>6. Conclusion</u>	57
<u>7. Acknowledgements</u>	59
<u>8. References</u>	60
<u>Report Documentation page</u>	64

Summary

Reactive nitrate transport in the Rabis Creek aquifer has been investigated by the application of numerical groundwater flow and geochemical solute transport models.

Groundwater flow	The groundwater flow simulations show that the flow is predominantly horizontal in most of the aquifer, but with downward or upward flow close to the water divide and the creeks, respectively.
Tritium transport	The tritium transport simulations show that the dispersivity values controlling dispersive mixing in the aquifer are small. However, on the time scales considered in this study (30 years) significant dispersion can take place. The simulations also indicate that the sharp nitrate and oxygen profiles found in the aquifer are due to fast reaction chemistry and not to low dispersive mixing.
Nitrate contamination	The reactive nitrate simulations show that the groundwater contamination problem at the site is groundwater flow controlled. The three-dimensional flow pattern results in an upper contaminated zone, while the deeper parts of the aquifer is nitrate-free due to the existence of reduction capacity (pyrite) in the aquifer. Nitrate is removed by oxidation of pyrite at the boundary (redox front) between the uncontaminated and contaminated groundwater. Nitrate is transported away laterally from the reaction zone, due to the nearly horizontal groundwater flow in most of the aquifer. A long-term simulation (to year 2050) indicates that more than 45% of the total mass of nitrate leached to the aquifer will be discharged to the creeks, while less than 40% will be removed by

denitrification. The relatively low concentrations of nitrate found in Rabis Creek can be explained from the simulations by a discharge of contaminated groundwater mixed with deep nitrate-free groundwater. The observations of the actual flow of groundwater to the creek, where groundwater trickles over the adjacent meadows, is probably responsible for a large reduction in nitrate concentrations (50% according to the simulations).

2. Danish summary

Denne rapport præsenterer hovedresultaterne fra modelberegninger af transport og omsætning af nitrat i grundvandsmagasinet ved Rabis bæk.

Transport og omsætning af nitrat er en funktion af flere samtidige fysiske, kemiske og biologiske processer. I denne sammenhæng er indflydelsen af den tre-dimensionale grundvandsstrøm (advektion), stof dispersionen og den kemiske/biologiske nitratreduktion på omfanget af nitrat forureningen søgt belyst.

Grundvands- strømning

Grundvandsmagasinet's mættede lagtykkelse varierer meget indenfor det undersøgte opland, men modelberegningerne viser, at størstedelen af grundvandstilskuddet strømmer af i den øvre del af magasinet med en meget lille vandtransport til de dybere dele.

Det er dog karakteristisk for dette grundvands-system, at afstrømningen til Rabis bæk består af grundvand fra både den øvre og nedre del af magasinet.

Dispersion

Den mekaniske opblanding eller hydrodynamiske dispersion, der sker i grundvandsmagasinet, og som hovedsagelig er forårsaget af geologiske inhomogeniteter er ikke særlig stor ved Rabis bæk. Modeleregninger af transport af tritium i grundvandsmagasinet og sammenligning med de faktiske observerede tritium koncentrationer viser, at specielt den transversale (dvs. vinkelret på strømrretningen) opblanding er meget lille. Dog vil dispersionen set over en lang tidshorisont (> 50 år) have en væsentlig betydning for transporten af nitrat, men i lighed med den ringe vertikale vandtransport vil den vertikale transport af nitrat være af mindre betydning.

Nitrat
forurening

Modelberegninger over transport og omsætning af nitrat, og hvor der tages hensyn til det tre-dimensionale strømningsmønster, stof dispersionen og nitrat fjernelse via oxidation af pyrit aflejringer, viser, at omfanget af nitratforurening af grundvandet og Rabis bæk, hovedsagelig er kontrolleret af selve grundvandsstrømningsmønstret og ikke så meget af kemiske/biologiske nitratreduktionsprocesser. Den karakteristiske grundvandsstrømning ved Rabis bæk med meget ringe vertikal vandtransport resulterer i en øvre forurennet zone, og en nedre nitrat-fri zone på grund af fjernelse af nitrat i dybder af ca. 10-15 m under grundvandsspejlet.

Modelberegningerne viser endvidere, at det grundvand der tilføres Rabis bæk, er en blanding af forurennet grundvand fra den øvre zone blandet med nitrat-frit grundvand fra den nedre zone. Sammenligninger med de gennemsnitlig observerede nitrat-koncentrationer i Rabis bæk indikerer, at selve tilstrømningen til Rabis bæk, via de tilstødende engarealer, bevirker en over 50% reduktion i nitratkoncentration.

Overordnet viser modelberegningerne, at lidt over en tredjedel af den samlede mængde nitrat, der tilføres grundvandsmagasinet, fjernes ved nitrat-reduktion, mens tæt ved halvdelen tilføres Rabis bæk med en efterfølgende halvering som følge af reduktionsprocesser i engarealerne.

3. Introduction

This report summarizes the results from application of numerical models to describing groundwater flow and transport of nitrate in the Rabis Creek catchment located in the western part of Denmark. The catchment has been selected as one of two research sites within the NPO-research programme. The two catchments represent two different, yet typical Danish aquifers. Engesgaard and Jensen (1990) report the results from the other catchment.

Nitrate contamination of unconfined aquifers

The unconfined aquifers in the western part of Denmark have increasing problems with nitrate contamination. A nitrate survey by Overgaard (1984) revealed a significant trend of increasing concentrations with time, with more than 10% of the wells exceeding the admissible level of 50 mg NO_3^-/l .

The vulnerability of the unprotected aquifers in this part of the country is dependent on a balance between the amount of nitrate leaching and the amount of nitrate removal by denitrification processes in the aquifers. The denitrification processes take place when nitrate oxidizes pyrite and lignite, which are both present in the quaternary glacial sand sediments. If nitrate leaching continues, this balance can change because the finite reserves of pyrite and lignite can be exhausted. Nitrate will then move unretarded through the aquifer.

Scope of the study

The primary objective of the project is therefore to quantify whether the balance between nitrate input and nitrate removal can be considered stable for the Rabis Creek catchment. In that perspective the report will discuss the dominant physical and chemical processes that affect this balance.

NPo modelling
studies

The objective is approached by simulating ground-water flow and reactive transport of nitrate at the local scale, i.e the Rabis Creek catchment scale (16 km²). In a modelling sense, the project is then closely related to that by Postma and Boesen (1990), who describe reactive nitrate transport at the streamline scale and that by Storm et al. (1990) who applied a regional scale model to evaluate the consequences of nitrate leaching at the Karup catchment scale (500 km²). Detailed modelling of the chemical processes has been carried out at the streamline scale, and the results were compared to the water chemistry observed at the site, whereas at the local and regional scale focus is on describing ground-water flow and transport processes in three dimensions coupled with a simple description of the nitrate reaction mechanisms.

Other modelling
studies

Only a few similar modelling studies have been found in the literature. Frind et al. (1989) applied a cross-sectional model incorporating an empirical kinetic nitrate degradation equation for pyrite oxidation to the Fuhrberger Feld aquifer. Similarly, Kinzelbach and Schäfer (1989) applied one- and two-dimensional models with kinetic nitrate oxidation of organic material. The present project and that of Storm et al. (1990) therefore appear to be the first attempt of a fully three-dimensional description of an aquifer nitrate contamination problem.

4. Methodology

This chapter describes:

- 1) The background
- 2) The model approach
- 3) The model tools

Although three-dimensional numerical groundwater flow and solute transport models have existed for the past two decades, the use of these models in field cases has been few in number. The reason has been the limited computer capacity in the past, but is today more constrained by the inadequacy of field data.

The present modelling effort is based on the compilation of field data by several institutions. The first section discusses the background for the present project in terms of the nitrate contamination problem at the site and the amount of field data available for three-dimensional modelling.

Since the inclusion of the third dimension, in relation to traditional two-dimensional models, and the incorporation of geochemical reactions create a new level of complexity, it is of paramount importance to have a detailed knowledge of the aquifer system and its behaviour. The second section therefore describes the model approach adopted in this study.

The third section describes briefly the various models that have been used.

4.1 Background

The Rabis Creek field site, Figure 1, is located in the western part of Denmark. Information about this area that pertains directly to this study will be given here. For more details, see Kristiansen et al. (1990) and Postma and Boesen (1990).

4.1.1 Hydrogeology

Geology

The aquifer consists of upper deposits of glacial outwash sands from the late - and post - Weichselian period underlain by prequaternary miocene deposits. The glacial sands are dominated by a medium-grained sand interbedded with local fine grained sand layers primarily in the upstream area. In the downstream area, medium- to coarse-grained sand layers appear (see Figures 2a and 2b in Kristiansen et al. (1990)). The distribution of these sand deposits can be interpreted as the result of depositions by braided rivers, both in a northward direction forming the Karup river valley with the medium-coarse sand deposits and in a more westernly direction causing deposition of fine to medium sands. The different sand deposits show little variation in grain size, and the aquifer can be characterized as being very homogenous with respect to lithology. The miocene deposits typically consist of micaceous sands and clays.

Aquifer geometry

The geometry of the aquifer with regard to the lower boundary is somewhat uncertain. In the mid- to downstream area, the aquifer bottom is found at depths of 15-20 m, while in the upstream area the exact location is unknown but is probably found at depths of more than 90 m, Kristiansen et al. (1990).

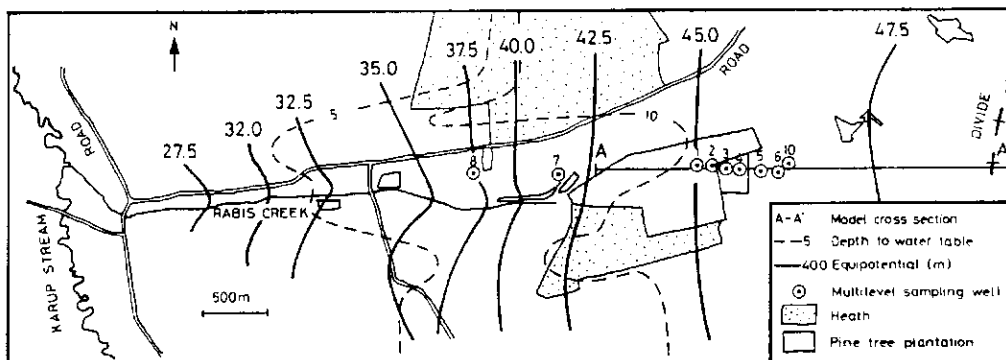


Figure 1
The Rabis Creek field site.

Rainfall and recharge

The average annual precipitation in the area was earlier (1970-80) found to be 790 mm with approximately half of the yearly precipitation recharging the aquifer (Miljøstyrelsen, 1983). At the climate station established as a part of the NPo-programme yearly precipitations of 874 mm and 761 mm were measured in 1988 and 1989 (Olesen, 1990).

Unsaturated flow

The depth to the water table aquifer can be up to 15 m in the upstream area. Andersen and Sevel (1974) found an average piston-like recharge propagation rate in the unsaturated zone of 3.5 m/month indicating a significant time lag between a rainfall event and actual recharge of the aquifer.

Groundwater flow

The groundwater flow patterns deduced from monthly observations in more than 25 wells (Kristiansen et al. (1990)) indicate two-dimensional horizontal groundwater flow from the water divide to Karup river. Generally, only small seasonal fluctuations in the water table are found (on the order of less than 1 m).

Rabis Creek Rabis Creek discharges most of the 16 km² research area. Discharge recordings at the surface gauging stations show very little variation over the year (Hansen (1990)).

Hydraulic parameter data Information about the hydraulic conductivities of the aquifer system is scarce. Miljøstyrelsen (1983) reported results from two short-term pump-tests where transmissivities of $4.4 - 5.8 \times 10^{-3}$ m²/s were calculated. These were estimated to correspond to a hydraulic conductivity of approximately 2×10^{-4} m/s.

4.1.2 Hydrogeochemistry

Land use and nitrate leaching Originally the area consisted of heath, but it is now primarily used for farming with only small areas of heath remaining and a pine tree plantation. The area was chosen specifically because it was possible to identify a nitrate plume below the plantation area by multi-level sampling in the six wells along a streamline trajectory.

Groundwater below arable land contains significant levels of nitrate, while groundwater derived from forested land is practically nitrate free, (Postma and Boesen (1990)).

The history of nitrate leaching is unknown, Postma and Boesen (1990), however established a simple historical long-term loading function based on the observed water chemistry which proved successful in their model application.

Aquifer geochemistry The aquifer can be divided into an upper, fully oxidized zone, 10-15 m thick, and a lower, reduced zone. The transition or oxidation-

reduction front separating the oxidized and reduced zone is characterized chemically by processes where first oxygen then nitrate oxidize pyrite (FeS_2) and organic material like lignite. Postma and Boesen (1990) found that only pyrite plays an active role in the oxidation-reduction (redox) processes.

Nitrate contamination of aquifer

The significance of the denitrification process as a natural occurring remediation against nitrate contamination relies on the fraction of nitrate leached to the aquifer and subsequently transported vertically to the redox front. Most of the transport of nitrate occurs laterally in the top one-third of the aquifer, and, with further depression of the redox front, the nearly horizontal flow in the aquifer will carry nitrate over the top of the reaction zone towards the creek. The problem of nitrate aquifer contamination at the site therefore appears to be groundwater flow controlled.

Nitrate contamination of Rabis Creek

Mixing of contaminated nitrate-rich and uncontaminated groundwater also occurs adjacent to Rabis Creek. Furthermore, the nitrate concentration in the discharge water to Rabis Creek is further reduced by denitrification when the discharge water trickles over the small meadows close to the creek, Kristiansen et al. (1990). Hansen (1990) found low levels of nitrate in the creek, although Brühsh and Bendix (1987) have found an increasing trend during the 60's, 70's and 80's.

Tritium

Tritium levels have also been determined in the transect of wells, Kristiansen et al. (1990). Some of the wells were deep enough to capture the distinct 1962-63 peak in tritium concentration.

4.2 The modeling approach

Factors determining nitrate transport

The movement of nitrate in soils and aquifers is governed by a complex interplay between time-dependent, simultaneous physical, chemical and biological processes.

To predict and quantify the effects of nitrate leaching on the groundwater and surface water systems the actual flow paths, flow velocities, dispersive mixing, and reactive mechanisms in the hydrogeological-geochemical system must be determined.

In a three-dimensional unsaturated - saturated flow system this becomes a complicated task. Some means of separating all these processes are necessary in order to identify the processes that ultimately control nitrate movement.

Modelling approach

This chapter is devoted to explaining the modelling strategy behind the present study in order to approach the problem in a manageable way. The modelling approach therefore involves three stages:

- 1) Determining flow paths and flow velocities in the system.
- 2) Determining soil and aquifer dispersive properties from simulating tritium transport.
- 3) Determining reactive mechanisms for nitrate transport.

Stage 1: Water flow

Stage 1 describes the model approach for determining unsaturated and saturated flow at the site. The two zones have been treated separately.

Unsaturated zone Since the water table is located from 1 to 15 meters below the soil surface, it is necessary to consider the transport of water (and solute) in the unsaturated zone. The technique for determining the seasonal and depth-dependent recharge flux to the groundwater region has been a combination of model simulations and use of already existing field experimental results.

Andersen and Sevel (1974) reported on their investigations at Grønhøj (2 km from the site) an average seasonal recharge flux velocity in the unsaturated zone of 3.5 m/month. The deep percolation will, like a piston-flow, on an average displace water in the profile with this velocity, and the depth to the groundwater table will thus determine the time lag between rainfall and actual recharge to the groundwater region.

Recharge regions To account for the variable depth to the groundwater table in the whole catchment the area was divided into three regions based on the depth to the groundwater table, see Figure 1. Region 1, 2 and 3 have 0-5 m, 5-10 m and 10-15 m depths to the water table, respectively.

Recharge flux The recharge flux was determined by applying the unsaturated zone model by Jensen (1983) to a hypothetical soil column incorporating realistic retention curves for sandy soils, and using the observations of rainfall and calculated values of potential evapotranspiration during the study

period (Olesen, 1990) as input. The recharge fluxes determined at the midpoints in the three regions (i.e. 2.5 m, 7.5 m and 12.5 m) were transformed to give monthly rates. This was assumed to be a sufficient resolution time scale for the groundwater model, which is calibrated against monthly observations of the groundwater table position.

Groundwater zone The nature of the groundwater flow pattern was investigated by a combination of two- and three-dimensional groundwater flow models. The two-dimensional areal and cross-sectional applications acted as preliminary analyses with the purpose of gathering as much experience as possible about the hydrogeological system before any fully three-dimensional applications were attempted. Since the latter represent the final results, the three-dimensional groundwater flow model will only be presented. Engesgaard(1988) illustrates the combined use of areal and profile flow modelling, and Keidser et al. (1990) use inverse modelling techniques for parameter estimation. The reader is referred to these references for information about the two-dimensional groundwater flow modelling.

Three-dimensional flow Although the groundwater flow field can be characterized as being almost horizontal with most of the flow taking place in the top one-third of the aquifer, a three-dimensional description of the flow paths and flow velocities is crucial when considering transport of nitrate. The vertical flux of nitrate to the oxidation-reduction front will determine how long denitrification will be active in the aquifer.

The geological-hydrogeological model given by Kristiansen et al. (1990) and the time-dependent

and average recharge flux along with proper specification of other boundary conditions are the basis for applying the model.

The model was used in a calibration and prediction phase. In the calibration phase only flow is considered, while in the prediction phase the flow model determines flow paths and velocities needed for predicting transport of tritium and nitrate.

Calibration phase In the calibration phase, the flow model was calibrated in transient state using monthly observations in 27 wells and flow discharge recordings in Rabis Creek.

Prediction phase In the prediction phase stationary flow was assumed. This is considered valid because the two transport simulations (tritium and nitrate) have a long time scale (> 30 years) whereas the seasonal variations in flow paths and flow velocities are less important compared to the uncertainties in e.g. the hydrogeological model or historical input of nitrate or tritium to the aquifer.

Stage 2: Tritium transport

Tritium as an
environmental
tracer

Tritium produced and released to the atmosphere from testing of thermonuclear bombs in the 50's and 60's has been used extensively as an environmental tracer in hydrological studies of water and solute transport in the subsurface.

Atmospheric fallout of tritium resulted in a very distinct concentration peak in the soil and groundwater environment which can be dated back to 1962-63 and which has been the basis for studies of e.g. groundwater recharge and solute

dispersion (Andersen and Sevel, 1974; Sevel et al., 1981; Egboka et al., 1983; Herweijer et al., 1985; Gvirtzman et al., 1988; and Robertson and Cherry, 1989).

In the present study, tritium profiles are used to estimate transport velocities and dispersive mixing in the unsaturated and saturated zone. The study is unique in the sense that it links vertical tritium transport through a deep unsaturated zone to that of near-horizontal tritium transport in the groundwater system.

Tritium in the
unsaturated zone

The investigation by Andersen and Sevel (1974) is used to estimate the effective velocity and the dispersive mixing in the unsaturated zone at the site. This study slightly reinterprets data from three of the wells used in their study.

Tritium in the
saturated zone

Tritium profiles in Wells 1, 2 and 10, figure 1, were used to estimate dispersive mixing in the groundwater region by applying a two-dimensional transport model in a cross-section along the transect of wells, figure 1. The mass flux of tritium to the water table zone was calculated on the basis of the investigations in the unsaturated zone.

Stage 3: Reactive nitrate transport

Nitrate removal
processes

To a certain extent are the possible impacts of nitrate leaching on the groundwater and surface water system controlled by removal of nitrate due to nitrate oxidation of pyrite. The problem therefore centres around a proper accounting for the depletion of the pyrite reserves in the aquifer. In essence, nitrate removal is

controlled by the amount of pyrite (reduction capacity) left in the aquifer, the location of these reserves, and the mass flux of oxidation potential (nitrate and oxygen) to these locations.

Modelling studies These observations are supported by the field data and modelling studies by Postma and Boesen (1990) and Engesgaard and Kipp (1990). The model by Engesgaard and Kipp (1990) was developed as a part of this project with the purpose of, in one dimension, accurately describing the rate of pyrite depletion and the ongoing chemical reactions at the oxidation-reduction front and also act as a verification model for developing a much more simplified nitrate reaction model, which could be incorporated into the three-dimensional groundwater flow and transport model. During the course of model development it was found that the application of a multi-dimensional version of the geochemical model (Engesgaard and Kipp, 1990) was not justified for several reasons. First of all, as discussed before, the problem at the catchment scale is mainly groundwater flow controlled; secondly, the denitrification reactions occur at specific locations (i.e. at the redox front) which would give excessive computer calculation workload if the comprehensive model were applied for the whole aquifer; thus requiring access to a vector computer processor.

Nitrate transport in the unsaturated zone In the unsaturated zone, oxygen is present at near-saturation levels, and nitrate is therefore transported as a conservative species. No chemical modelling is therefore attempted here.

History of nitrate leaching The history of nitrate leaching is unknown. Postma and Boesen (1990) used a simple relation based on the observed water chemistry. A similar approach will be used here. However, because of

the great uncertainty in estimating the history of nitrate leaching, no actual routing of nitrate through the unsaturated zone was performed.

4.3 The modelling tools

Several modelling tools have been in use in order to simulate water flow, tritium transport, and reactive nitrate transport at the Rabis Creek field site.

This chapter is devoted to giving the necessary description of the various models and will provide the basis for a complete understanding of the modelling approach and the modelling results.

Some of the models represent new developments, while others have been modified to suit the present purpose, and again others have been used on an as is basis.

4.3.1 Flow models

Unsaturated zone Flow in the unsaturated zone and recharge to the groundwater region have been determined by applying the unsaturated zone model developed by Jensen (1983). In one dimension the model solves the Richards equation given by

$$C \frac{\partial \psi}{\partial t} = \frac{\partial}{\partial z} \left(K \frac{\partial \psi}{\partial z} \right) - \frac{\partial K}{\partial z} - S \quad (4.1)$$

where

ψ = capillary pressure (L)

C = water capacity (L^{-1})

K = hydraulic conductivity (LT^{-1})

S = sink term representing uptake by roots (T^{-1})

z = vertical coordinate
(positive downwards) (L)

t = time (T)

Rainfall measured at the climate station provided the upper flux boundary condition, while the lower boundary condition was zero pressure at a water table fixed at 15 m depth. Recharge was calculated at depths of 2.5 m, 7.5 m and 12.5 m corresponding to the midpoints in the recharge regions discussed in section 4.2 and shown in Figure 1. The recharge function was only used during the groundwater flow calibration phase. In the prediction phase, stationary flow with an average recharge of 385 mm/year was assumed. Andersen and Sevel (1974) calculated an average value of 383 mm/year for the period 1961-72, while Miljøstyrelsen (1983) found a value of 375 mm/year for the period 1968-76.

Groundwater flow model	The three-dimensional groundwater flow model is a descendant of the HST3D model (Kipp, 1987). The
HST3D model	HST3D model is able to account for simultaneous heat (H) and solute (S) transport (T) in a three-dimensional (3D) variable-density groundwater flow system.

Since the effects of heat transport and variable-density flow are negligible for the groundwater flow system at the Rabis Creek field site, it was decided, in cooperation with Kenneth Kipp, to tailor the model to the needs of this project.

In addition to removing all the heat transport and variable-density calculations, a new direct equation solver was installed, the iterative solver was modified, and a more flexible free-surface condition for water table aquifers was developed.

ST3D model	The new model, now called ST3D, solves the governing three-dimensional groundwater flow equation:
------------	---

$$\frac{\partial}{\partial x}(K_x \frac{\partial h}{\partial x}) + \frac{\partial}{\partial y}(K_y \frac{\partial h}{\partial y}) + \frac{\partial}{\partial z}(K_z \frac{\partial h}{\partial z}) = S \frac{\partial h}{\partial t} \quad (4.2)$$

where

h = hydraulic potential (L)
 K_x, K_y, K_z = hydraulic conductivities (L/T)
in the x, y and z directions
S = specific storage (L^{-1})
x, y and z = space coordinates (L)

To solve equation (4.2), given proper spatial specification of hydraulic conductivities and specific storages, requires a set of boundary conditions. The options for specifying boundary conditions in HST3D are also available in ST3D, but now with a more flexible water table boundary condition, allowing a water table to transverse several numerical grid layers.

4.3.2 Tritium transport models

The programme CXTFIT (Parker and van Genuchten, 1984) has been used to simulate tritium transport in the unsaturated zone.

CXTFIT model

The programme uses a non-linear least-squares inversion method to automatically fit an analytical solution of the advection-dispersion equation including radioactive decay to a set of observation points. The equation is given by;

$$\frac{\partial C}{\partial t} = D \frac{\partial^2 C}{\partial x^2} - v \frac{\partial C}{\partial x} - \mu C \quad (4.3)$$

where

C = resident or flux concentration
(Tritium units, TU)
D = dispersion coefficient
= $D_L \times v (L^2 T^{-1})$
 D_L = dispersivity (L)
v = interstitial velocity (LT^{-1})

μ = first-order rate constant (T^{-1})
x = distance (L)
t = time (T)

An option in the model allows the user to bypass the optimization method and use the program as a simple analytical solution to equation (4.3).

Resident concentrations are volume-averaged concentrations (e.g. from measurements on soil samples), and flux concentrations are flux-averaged concentrations (e.g. from measurements at the outlet of soil columns). The two concentration detection modes obey the same equation, but with a different top boundary condition, see Parker and van Genuchten (1984)

In the optimization method the user selects which parameters shall be variable. In this application only D and V are optimized, since μ , the decay constant, is known a priori.

Given a set of observation points the program will then optimize a match by a solution of equation (4.3) by varying V and D. The output is an optimum V and D and their 95% confidence intervals.

MOC model

In the groundwater region the MOC model (Konikow and Bredehoeft (1978)) has been used in a cross-section close to the transect of wells, see Figure 1. The ST3D model used for groundwater flow was not used, because it is based on a numerical finite difference technique to solve the transport equations, which suffers from numerical dispersion unless very small mesh sizes are employed. In relation to estimating dispersive mixing in the groundwater region, the use of ST3D becomes less attractive because of excessive numerical dispersion with feasible mesh sizes. The

MOC model, on the other hand, uses a particle-tracking method which is free of numerical dispersion. The MOC model has also been used for preliminary groundwater flow predictions, Engesgaard (1988) and Keidser et al. (1990).

The MOC model has in the literature primarily been used for areal simulations, but has the possibility of being applied in a cross-section for artesian aquifers. For the water table aquifer at Rabis Creek where the simulated water table possibly can traverse grid layers, some modifications were necessary concerning the determination of flow velocities. The details, however, will not be presented here.

4.3.3 Reactive nitrate transport models

As discussed in the model approach two quite different types of reactive nitrate transport models have been used.

1-D geochemical model

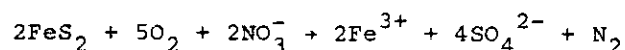
The first model is described in detail by Engesgaard and Kipp (1990) and only a brief summary will be given here. The model is based on a coupling between a classical finite-difference solution to several one-dimensional transport equations and a chemical equilibration programme, PHREEQE, Parkhurst et al. (1980). The role of the first step of solving transport is to track the movement of multiple components (i.e. multiple solutions to the transport equation) providing the total aqueous component concentrations needed by the chemical equilibrium code before any equilibrium speciation in the second step can be car-

ried out. The model is flexible in that it can take an arbitrary number of components, species, and minerals. Special considerations have been given to the problems of simulating the movement of sharp mineral fronts and redox processes, because physical and chemical processes at the site determine the redox-controlled movement of sharp pyrite fronts. A sequential iteration between the two calculation steps maintains the sharp fronts. For redox processes, a mass conservation equation for the redox state is written for both the transport and the chemistry step. The reader is referred to Engesgaard and Kipp (1990) for more details.

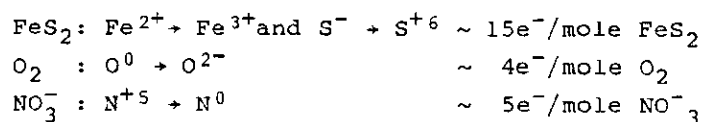
As discussed in section 4.1, the problem of nitrate contamination appears to be groundwater flow controlled. Determination of the three-dimensional groundwater flow paths and velocities therefore seems more important than detailed calculations of the chemical speciation of the various components in the aquifer. A simple nitrate reaction model has therefore been incorporated into the ST3D model.

3D hydrogeo-
chemical model

At the redox front the following reaction between oxidizing and reducing agents can take place:



Here, the following transfer of electrons takes place (changes in oxidation states);



It is seen that 2 mole $\text{FeS}_2 \times 15\text{e}^-/\text{mole FeS}_2 = 30\text{e}^-$ donated by pyrite is accepted by oxygen and nitrate in that 5 mole $\text{O}_2 \times 4\text{e}^-/\text{mole O}_2 + 2 \text{ mole NO}_3^- \times 5\text{e}^-/\text{mole NO}_3^- = 30\text{e}^-$.

Simple nitrate
reaction model

Instead of considering oxygen and nitrate as two different species one might treat them together as one single species, an oxidation potential species, X. The chemical reaction can then be written in a simplified form as:



From here on the products will not be discussed. To account for the oxidation-reduction processes, the concentration of the oxidation potential should then be given as equivalents/l. The concentration of X is then given as;

$$X = \frac{1}{2} (5[4 \times C_{\text{O}_2}] + 2[5 \times C_{\text{NO}_3^-}])$$

The factor of $\frac{1}{2}$ comes from formulating the last reaction in terms of one mole FeS_2 only. C_{O_2} and $C_{\text{NO}_3^-}$ are the molar concentrations of oxygen² and nitrate, respectively. Pyrite and oxidation potential can then react on an equivalent basis, based on the transfer of electrons. In essence, only simple bookkeeping is needed of the electron transfers. If no pyrite is left in a given cell, the reaction is automatically turned off. A similar scheme for instantaneous degradation of organic contaminants is presented by Rifai and Bedient (1990). An important element in this simple model is the a priori location of the pyrite reserves, i.e. specification of the depth to the redox front in the whole aquifer.

5. Results

5.1 Flow

Recharge

Recharge to the groundwater region has been calculated by the unsaturated model, described in section 4.3, at three depths, 2.5 m, 7.5 m and 12.5 m, based upon available rainfall and potential evapotranspiration data. The results are shown in figure 2.

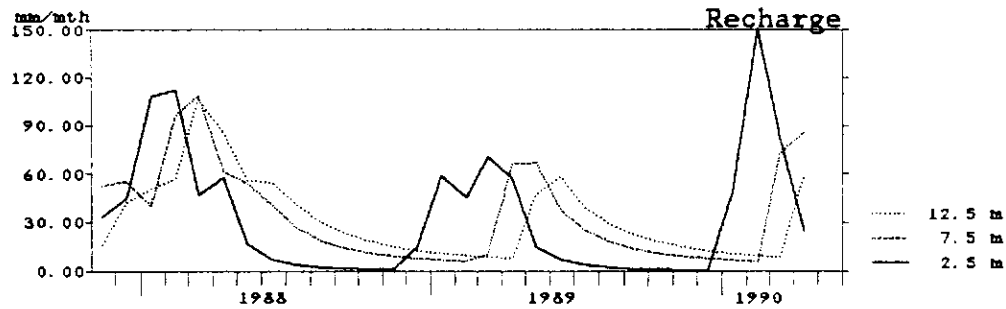


Figure 2

Calculated recharge to the groundwater table at three depths.

Recharge propagation velocity

The winter period of 1988-89 had a lower total recharge than the two other winters, and the summer of 1989 was very low in rainfall resulting in a long period with practically no recharge. During the first months of 1990 high rates of recharge have been calculated. The front propagation velocity between the 2.5 m and 7.5 m depths is in the range of 2.5 - 5.0 m/month. Between the 7.5 m and 12.5 m depths the range in velocity is from nearly zero to 2.5 m/month. Andersen and Sevel (1974) found an average rate of 3.5 m/month for a 22 m deep profile.

This value is somewhat higher than the average rate found in this study.

Groundwater flow The ST3D model has been calibrated using the transient recharge function and the hydrogeological information available, see section 4.1. Equal discretization of 400.0 m and 300.0 m in the two horizontal directions was used, while variable spacing of 5.0 m to 12.5 m was used in the vertical direction. Trial runs with double grid density in the horizontal directions showed no major improvements in the flow simulation results, probably in consequence of the homogeneity of the aquifer and the small water table fluctuations.

Four types of sediments have been introduced in the three-dimensional aquifer; fine, medium and coarse sands and clays.

The results will be presented as time-series of observed and final calculated water tables in eight wells and observed and final calculated average annual discharges at the Birthesminde surface water-gauging station. The location of the wells is shown in Figure 5.

Hydraulic
conductivities The hydraulic conductivities were $1 \cdot 10^{-4}$, $2 \cdot 10^{-4}$ and $9 \cdot 10^{-4}$ m/s for the fine-, medium- and coarse-grained sands and $1 \cdot 10^{-7}$ m/s for the clays. The values for the sand sediments correspond to those found in Miljøstyrelsen (1983) and Keidser et al. (1990). Anisotropy in the hydraulic conductivities was only present in the horizontal to vertical direction and was estimated in the range 25-50 for the sand layers. The porosities were set at an average 35% in the whole simulation region.

Simulated response The final calibration and observations for the in eight wells eight wells are shown in Figures 3 and 4. For some of the wells a discrepancy is present between the simulation and observations at the start of the simulation. This is primarily due to difficulties in estimating the initial water table, but is also related to the spatial discretization where the calculated value represents the mean over an area of 400 by 300 m, while the observed value essentially represents a point

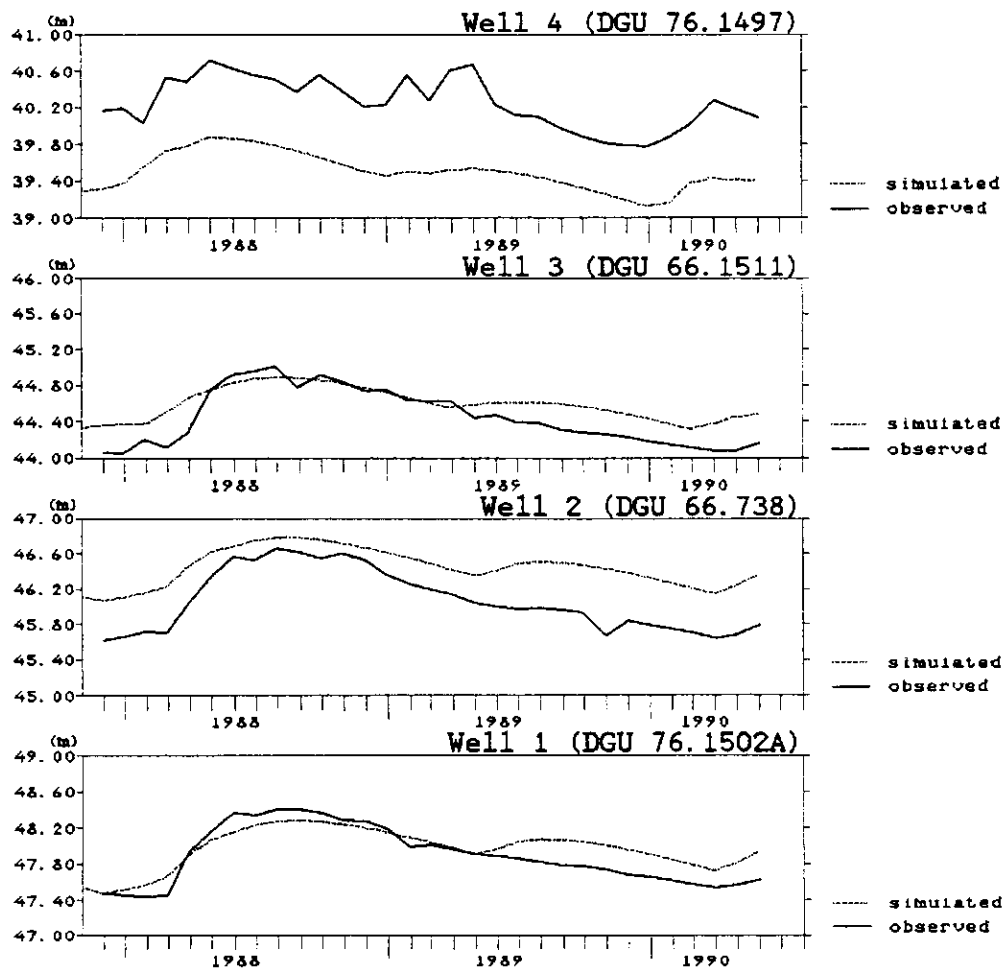


Figure 3
Time series of observed and simulated water table levels for wells 1 - 4.

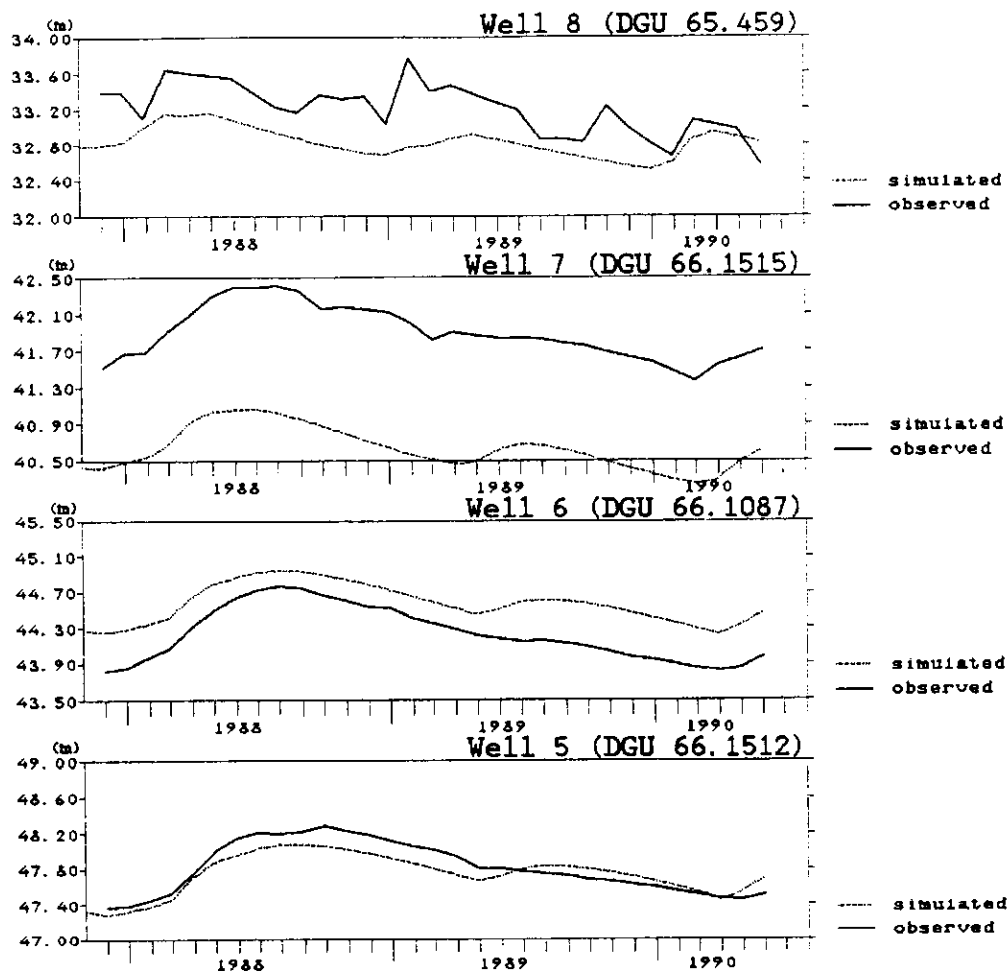


Figure 4

Time series of observed and simulated water table levels for wells 5 - 8.

value. It is therefore the dynamic response rather than the absolute values which should be compared. In the two downstream wells, (4 and 8), the water table fluctuates more than simulated. This can be due to slightly wrong definitions of the recharge regions.

Generally, there is good agreement between the simulation results and the observations. The predicted increase in water table level in 1988 is too low, while, on the other hand, the predicted increase in 1989 is not observed. These discrepancies are judged as being caused by a slightly wrong recharge function.

Discharge to
creek

The observed annual mean discharge in Rabis Creek at Birthesminde was 133.0 and 114.0 l/s in 1988 and 1989, respectively (Hansen, 1990). The simulated discharge of 141.0 and 125.0 l/s in 1988 and 1989 are in good agreement with the observations indicating that the flow to the creek is simulated correctly.

Figure 5 shows the simulated and observed water table contours for March 1989. Generally, there is good agreement. The disagreement close to the creek should not be taken into account, because the almost straight observed water table contours

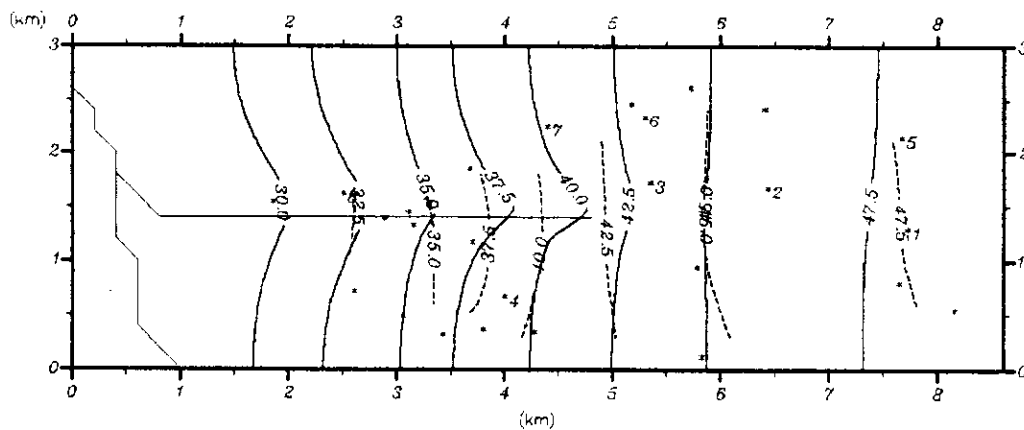


Figure 5
Observed and simulated water table contours (m)
March 1989. The observation wells are shown as a
*. The numbered wells correspond to those in
Figures 3 and 4.

close to the Rabis Creek are due to lack of information about the water table in that area.

Groundwater
paths

Figures 6a and 6b show calculated flow velocity vectors in a profile along the transect of wells and 1 km south of it, respectively. Note that the figures are not to scale. Significant downward and upward flow is present at the water divide and close to Rabis Creek, respectively. In Figure 6a, an impermeable clay layer results in practically zero flow velocities in the middle of the profile.

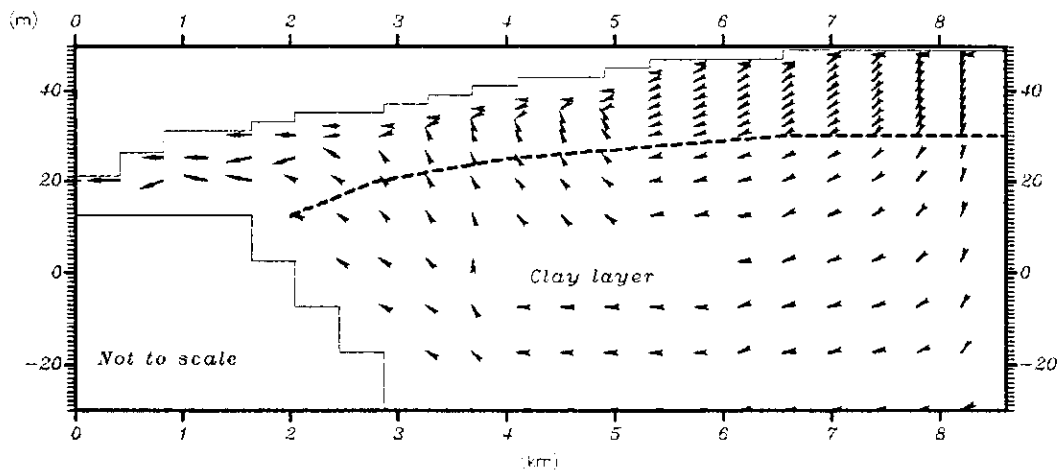
The velocity vectors indicate that most of the flow takes place in the top one-third of the aquifer i.e. at elevations higher than 20-30 m. The redox front is located approximately at these elevations as shown in Figure 6. The vertical flow component is very small close to the redox front.

5.2 Tritium transport

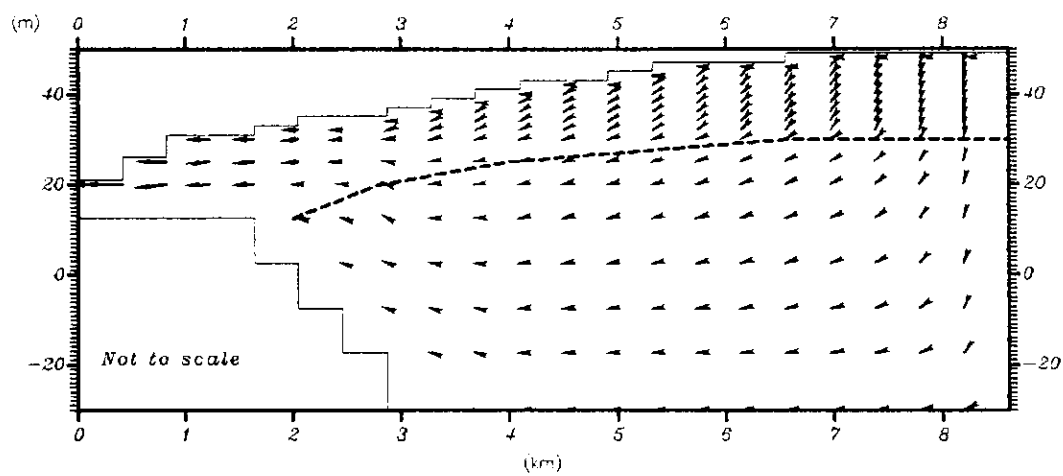
Three out of the four tritium profiles obtained by Andersen and Sevel (1974) are used to investigate the long-term effective advective and dispersive processes in the unsaturated zone. The profiles were obtained at two-year intervals from 1966-1972. The last profile from 1972 was not used because the 1962-1963 peak has left the unsaturated zone.

Andersen and
Sevel investi-
gation

Two simple models were used by Andersen and Sevel (1974) to determine vertical transport velocities and dispersive mixing (a displacement model with and without dispersion). Both models were based



(a)



(b)

Figure 6

Calculated velocity vectors at the transect of wells (a) and 1.0 km south of it (b). Each velocity vector represents a computational node point. No attempt has been made to scale the velocity vectors properly. The redox front is shown as a dashed line.

on simple recharge calculations and a tritium input function at the ground surface. Data on precipitation and soil moisture were collected at the site or close to the site, while data for tritium in precipitation came from stations in Sweden and West Germany, and during the period 1962-68, from Ødum only 50 km from the site.

Variation in
percolation rate

The greatest limitation of CXTFIT is the assumption of a constant velocity in the vertical direction. Since the percolation rate during the six year period naturally showed a seasonal variation (e.g. zero in the summer period), and because the deep unsaturated zone contains several yearly tritium pulses, the usefulness of CXTFIT may seem limited. However, use of CXTFIT can be justified since the purpose here is to study the long-term effective advective-dispersive processes, and the year-to-year variations in recharge hence become less significant.

Non-volume and
volume-based
tritium input
function

In the first method, six months averages of tritium concentrations were calculated based on monthly values of the measured tritium content in precipitation (Sevel, Pers.Comm.). These were non-volume averages meaning that they were not weighted according to the ratio of monthly percolation and average percolation during the six months. The non-volume based tritium input function is given in Figure 7. In the second method, a volume-based tritium input function was used. Instead of calculating new six-months average tritium concentrations, the time scale of the input function was changed instead by the method described below.

The time-averaged percolation $\langle q \rangle^*$ can be calculated as:

$$\langle q \rangle^* = \frac{1}{t_m} \int_0^{t_m} \langle q \rangle(\tau) d\tau$$

where t_m is the time interval of interest, and $\langle q \rangle$ represents the time-dependent percolation. A new time scale, t^* , for the tritium input function can be established by weighting the cumulative percolation to the average percolation according to

$$t^* = \frac{\int_0^t \langle q \rangle(\tau) d\tau}{\langle q \rangle^*}$$

On a half year basis, high and low percolation rates are then given more and less weight, respectively.

Resident and flux concentration models The programme CTXFIT was used in two ways. First, the programme was used in resident concentration mode to obtain effective transport velocities and dispersion coefficients by fitting solutions to equation (4.3) to the tritium profiles. Next, the optimization procedure was bypassed, and flux concentrations were predicted at several depths. The temporal variation in flux concentrations at these depths then represents the mass flux of tritium to the groundwater system.

Optimized values All the results from the automatic fitting procedure are given in Table 1, and some of the results are shown in Figure 8. The optimized values of velocity and dispersion coefficients were found by using data from each well individually (single wells) and data from two different combinations of the three wells (multiple wells) with the real (t) or transformed timescale (t^*). The 95% confidence limits and correlation coefficients are also given.

The single well results gave effective vertical velocities in the range 2.60 - 4.43 m/year and dispersion coefficients in the range 3.4 - 26.9 m/year. The fit for Well 4 was very poor ($r = 0.31$ and 0.49) which is due to the very flat peak

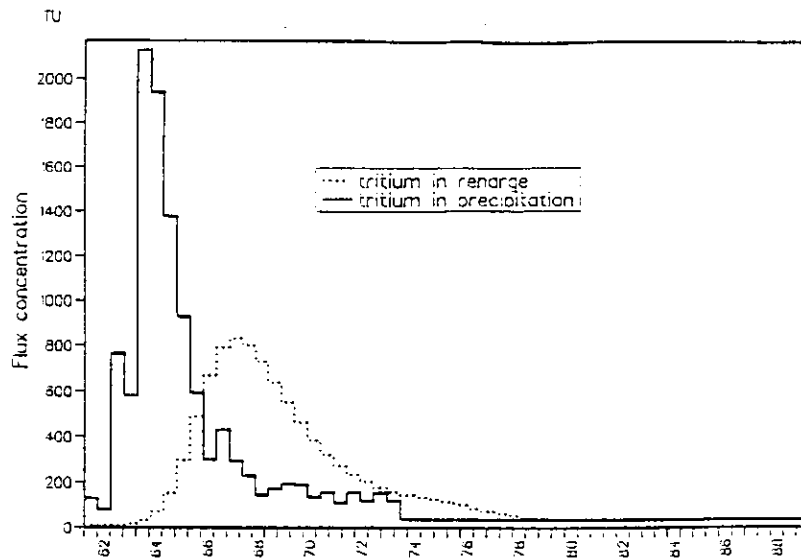


Figure 7

Tritium input functions at the ground surface (based on Andersen and Sevel (1974)) and at the water table located at 14 m depth.

Well no.	Time scale	$V_z \pm \sigma (\text{m/y})$	$D \pm \sigma (\text{m}^2/\text{y})$	r
1		3.47 ± 0.20	4.75 ± 1.37	0.88
4	t	3.00 ± 1.41	26.9 ± 34.72	0.31
5		4.42 ± 0.50	3.40 ± 4.45	0.77
1		3.35 ± 0.18	4.27 ± 1.26	0.87
4	t*	2.60 ± 0.50	10.95 ± 7.73	0.49
5		4.43 ± 0.45	3.63 ± 4.28	0.77
1+4+5		3.34 ± 0.25	7.29 ± 2.23	0.76
1+5	t	3.58 ± 0.19	4.90 ± 1.34	0.88
1+4+5		3.27 ± 0.24	6.44 ± 1.92	0.78
1+5	t*	3.48 ± 0.18	4.45 ± 1.26	0.87

Table 1

Results of the CXTFIT model for wells 1, 2 and 5 from Andersen and Sevel (1974). t and t* reflect real and transformed time scale, respectively. $\pm \sigma$ is the 95% confidence limit. r is the correlation coefficient.

in the tritium profile, Figure 8, causing CXTFIT to predict an unrealistically high value of the dispersion coefficient. Andersen and Sevel (1979) had difficulties also when fitting their models to the Well 4 data. The transformed time scale has little effect on the optimized values except for Well 4 where the velocity and dispersion coefficients were predicted lower for the transformed time scale. If a monthly based tritium input function had been used instead, larger differences in the results can be expected.

In Table 1 are also listed the optimized parameters obtained by including data from more than one well in the optimization process. Two combinations have been used; one includes data from all three wells the other omits data from Well 4. The results are similar to those for the single Well 1 indicating that this well plays a major role in the optimization. The transformed time-scale again has little effect on the results.

Effective values

The results from the single Wells 1 and 5 were used to calculate an effective velocity and dispersion coefficient. A simple mean of the two results yielded a vertical velocity of approximately $V_z = 4$ m/year and a dispersion coefficient of approximately $D = 4$ m²/year. The longitudinal dispersivity in the unsaturated zone is thus $D_L = D/V_z = 1$ m. Andersen and Sevel (1974) report values for the vertical velocity and dispersion coefficient of 4.5 m/year and 3.2 m²/year, respectively. The reasons for the high dispersivity are probably due to a combination of transient flow conditions and geological heterogeneity. The changes in percolation rates over the season will disperse the tritium profile, and consequently a higher dispersivity is expected.

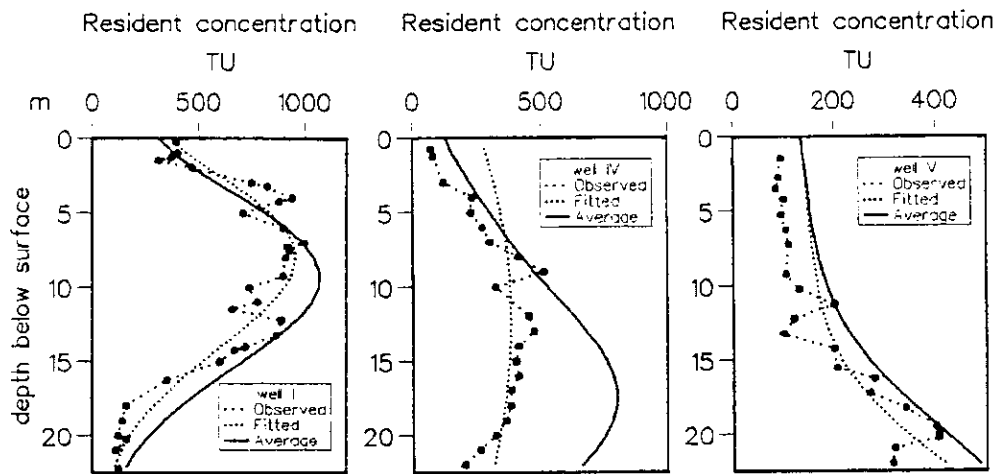


Figure 8

Observed (from Andersen and Sevel (1974)) and calculated (fitted and average) tritium profiles in Well 1, 4 and 5.

Figure 8 shows the results for Wells 1, 4 and 5 for the non-volume based tritium input function. The profile obtained on the basis of the optimized parameters and the profile calculated with the mean velocity and dispersion coefficient are shown along with the observed profile. For Well 1 and 5 the two predicted profiles have the same shape, whereas they differ significantly for Well 4.

Flux of tritium
to aquifer

The mean velocity and dispersion coefficient were used to calculate the flux tritium input to the aquifer at a depth of 14 m. This depth is representative for the unsaturated zone at the transect of wells. The result is shown in Figure 7. It is evident that the unsaturated zone has a significant effect on the tritium flux to the aquifer. The peak concentration is almost one-third of that measured in precipitation due to dispersion and decay in the unsaturated zone.

Tritium transport in groundwater The MOC model described in section 4.3.1 was used to describe the transport processes in the groundwater region in a cross-section close to the transect of wells. The cross-section is shown in Figure 1. The analysis has been carried out by a parameter sensitivity study of the longitudinal and transverse dispersivity values. Furthermore, the analysis provides a validation of the hydraulic conductivity distributions obtained from the flow calibration.

The cross-section was discretized into 40 m by 1 m cells in the horizontal and vertical direction, respectively. Stationary flow conditions were assumed based on a recharge of 385 mm/year, a downstream specified head boundary of 43.0 m and a no-flux upstream boundary in the cross-section A-A' shown in Figure 1. The tritium input function at the groundwater table was estimated by the procedure discussed above. Hydraulic conductivities of $2.2 - 2.9 \cdot 10^{-4}$ m/s were used to obtain a water table that approximately matched the field observations at the transect of wells. The hydraulic conductivities correspond closely to those determined in section 5.1.

Results from simulations with three combinations of longitudinal and transverse dispersivities are shown in Figure 9.

The low dispersive mixing case (D_L and D_T equal to zero) clearly overpredicts the 1962-63 peak by close to a factor of two. The large dispersive mixing case ($D_L = 5$ m and $D_T = 0.25$ m) results in a profile with no peak at all. The intermediate case ($D_L = 0.5$ m and $D_T = 0.005$ m) compares well with Well 2 and Well 10 as far as the magnitude of the peak is concerned, while Well 1 is over-

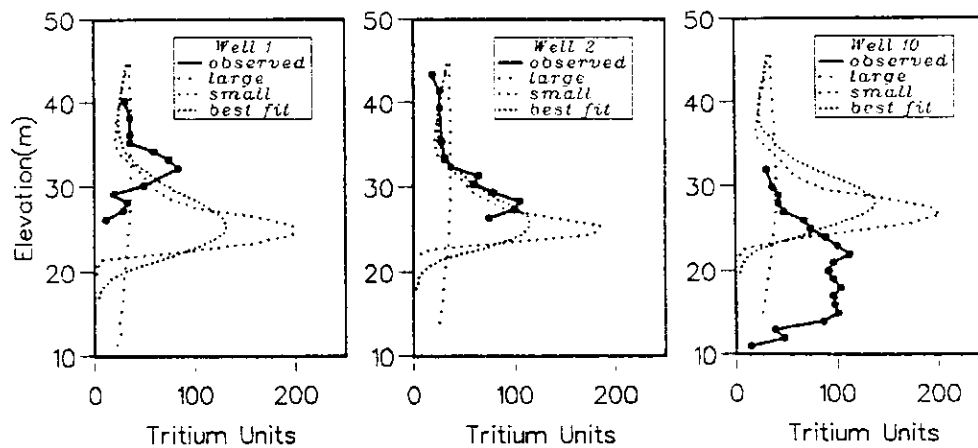


Figure 9

Observed and calculated tritium profiles in Wells 1, 2 and 10.

predicted. In none of the three wells is the vertical position of the peak simulated correctly. The observed profiles indicate a strong vertical flow upwards from Well 10 where the peak is located approximately at an elevation of 18.0 m to Well 1 where the peak is located 15.0 m higher. The change in the vertical location of the peak occurs over a distance of less than 1 km. The model was unable to reproduce this quite significant upward flow. The reasons for the lack of agreement can be the presence of impermeable clay layers somewhere between Wells 1 and 10, reduced recharge below the plantation, and the influence of the creek. The most probable cause is the appearance of isolated clay layers which are known to exist in the aquifer. This is especially the case close to the transect of wells as demonstrated in Figure 6a showing the flow pattern at the transect of wells. There are indications that the

clay layer present in this profile may extend further upstream and thereby come closer to the transect of wells (Well 9 in Figure 2b of Kristiansen et al., 1990). Figure 6a also shows the influence of Rabis Creek on the flow pattern. However, the effect is probably only minor at the wells. A 15% reduction in recharge at the plantation was used in the simulation. Much higher reductions are not likely.

Even with these discrepancies it has been demonstrated that small dispersivities of the order of 0.5 m and 0.005 m for longitudinal and transverse dispersivities, respectively, can cause significant dispersion in the aquifer.

5.3 Reactive nitrate transport

The distribution of nitrate in the Rabis Creek aquifer and the amount discharged to the creek are a function of how much of the nitrate is transported to depths where nitrate are removed by denitrification and how much will be carried over the top of the reaction zone and discharged directly to Rabis Creek.

Quantitative predictions of the depletion rate of reduction capacity (vertical movement of the redox front) and the amount of contact between nitrate and reduction capacity (e.g. fraction of leached nitrate to that removed) are needed in order to evaluate the impacts of nitrate leaching on the Rabis Creek aquifer.

5.3.1 Rates of redox front movement

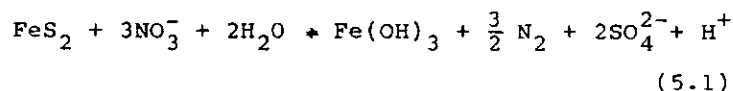
The basis for evaluating the rates of redox front movement has been given by Engesgaard and Kipp (1990). Only a brief summary will be given here, with an additional discussion of the sensitivity of the removal rates against variations in chemical and physical parameters.

1-D example

The example considers nitrate and oxygen oxidation of pyrite in a one-dimensional streamtube crossing the redox front. The example is based on introducing a contaminated inlet solution at a representative groundwater flow rate to an initially uncontaminated reduced solution. The inlet and initial solutions were specified with some reference to the observed water chemistry at the site.

Oxidation of pyrite

Nitrate and oxygen oxidize pyrite according to



In Equation (5.1), all Fe^{2+} from the pyrite dissolution will precipitate as $\text{Fe}(\text{OH})_3$, which might not be the case. However, this is considered by the model, and Equations (5.1) therefore represent only that fraction of Fe^{2+} released from pyrite dissolution that will be oxidized further and precipitated as Fe^{3+} in $\text{Fe}(\text{OH})_3$.

Organic material

The influence of organic material was neglected in this simulation, because the total inorganic carbon concentrations show little variation across the front, as discussed by Postma and Boesen (1990). The reaction time scale for oxidation of organic material is believed to be so high that it does not affect the water chemistry significantly.

The geochemical model by Engesgaard and Kipp (1990) is based on equilibrium chemistry. The applicability of this type of model to the chemical reaction system in the Rabis Creek aquifer can be questioned, of course. A general criterion for assuming equilibrium, the local equilibrium assumption (LEA), is that the rates of all chemical reactions are much faster than the rate of solute transport.

No chemical reaction mechanisms or rate constants for the geochemical processes governing nitrate transport at the Rabis Creek field site are known. The best source of information about the validity of the LEA then comes from the nitrate and oxygen profiles in the transect of wells. Postma and Boesen (1990) report that these are very sharp, indicating that the reactions are fast compared to the rate of transport.

If a kinetic reaction rate governed the redox-controlled precipitation-dissolution processes, a more dispersed profile would be expected. Kinzelbach and Schäfer (1989) give an example of a dispersed profile as a result of kinetic degradation of organic material. Frind et al. (1989) also observed sharp nitrate profiles due to oxidation of pyrite. However, they chose a kinetic model and explained the sharpness of the profile as caused by very low transverse dispersion rates (on the order of molecular diffusion).

The tritium transport simulations showed that with zero transverse dispersion the model was unable to reproduce the observed tritium profiles in Wells 1, 2 and 10. We therefore conclude that the sharpness of the nitrate and oxygen profiles is caused by fast chemical reactions, and that an equilibrium-based model is a valid approximation for this chemical reaction system.

	Solution	
	<u>Contaminated</u>	<u>Uncontaminated</u>
pH	5.70	8.67
pE	16.53	-4.30
Ca ²⁺	18.0	36.3
Mg ²⁺	10.0	2.0
Na ⁺	14.4	14.0
Cl ⁻	24.0	19.0
Fe	$6.7 \cdot 10^{-3}$	4.4
CO ₃ ²⁻	16.8	78.1
SO ₄ ²⁻	28.0	33.6
NO ₃ ⁻	65.0	0
FeS ₂	-	431.9
Fe(OH) ₃	-	0

Table 2

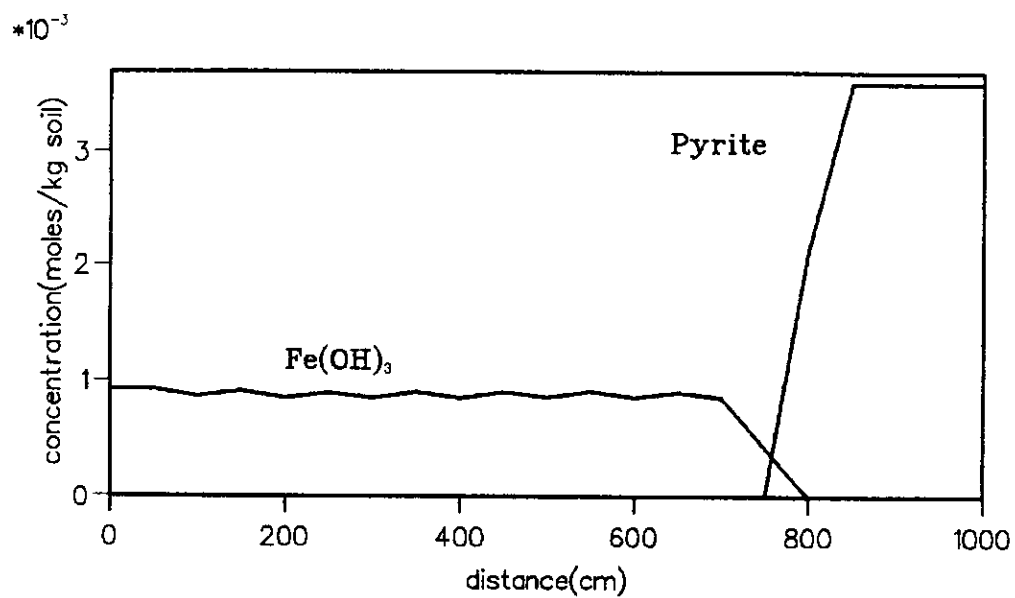
Total concentrations of aqueous components (mg/l) and minerals (mg/kg soil) in contaminated and uncontaminated solution.

Inlet and initial solutions From well water samples above and below the redox front, representative inlet boundary and initial conditions were established. These are shown in Table 2.

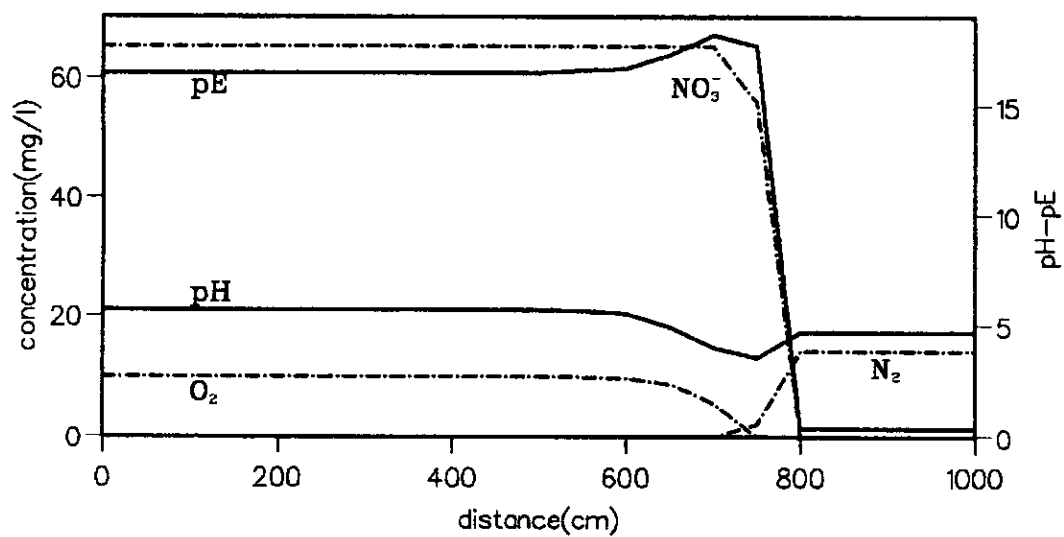
The pE in the contaminated solution was found by adjusting the pE until the concentration of dissolved oxygen was 10 mg/l, which match the conditions found in the oxidized zone.

The interstitial velocity was set at 25 m/year for this example, representative for the condition at the nitrate plume.

Redox front movement The calculated results are presented as spatial profiles after a simulation time of 20 years, Figures 10 and 11. Figure 10a shows the mineral distribution. After 20 years the pyrite front has

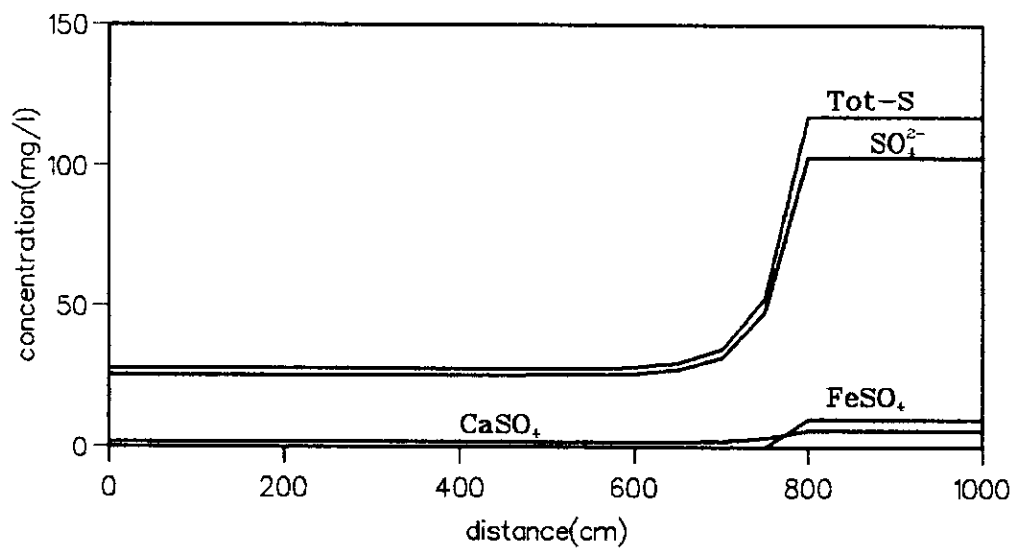


(a)

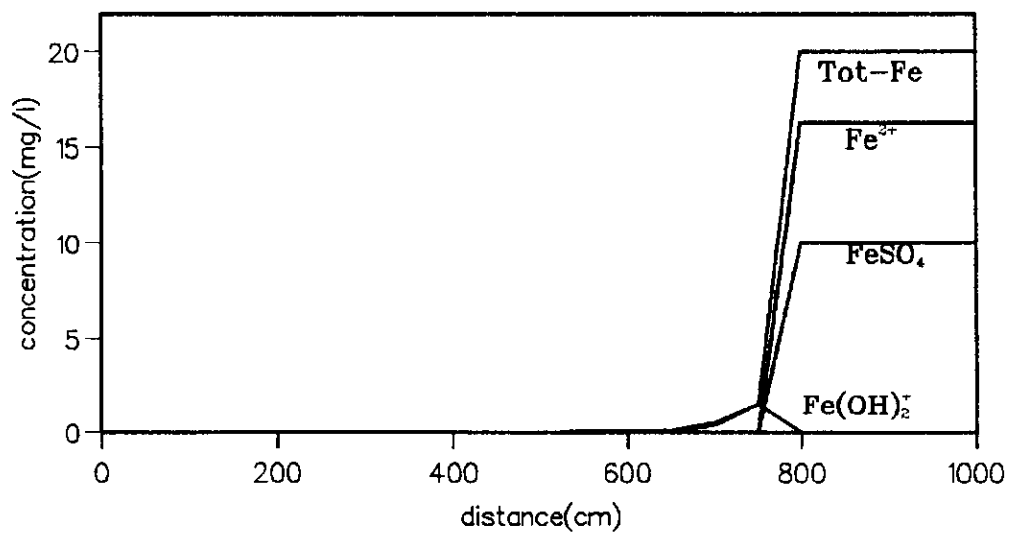


(b)

Figure 10. Mineral distribution (a) and concentration profiles (b) at $t = 20$ years.



(a)



(b)

Figure 11. Spatial profiles of species in the sulphur (a) and iron (b) system at $t = 20$ years.

moved to a location of approximately 800 cm. The average rate of front movement is thus 40 cm/year under the given conditions. As pyrite dissolves, part of the Fe^{2+} is oxidized and precipitates as $\text{Fe}(\text{OH})_3$.

Figure 10b shows the pE, pH, O_2 , NO_3^- and N_2 distribution. Upstream from the front, O_2 and NO_3^- are present and they disappear quickly close to the front, although the O_2 profile is more dispersed due to the pE conditions approaching the front. Close to the front, both NO_3^- and N_2 are present.

Figures 11a and 11b show the distribution of some of the major redox species. The SO_4^{2-} ion is the major species in the sulphur system. In the iron system, Fe^{2+} is the dominant species.

The average rate of front movement (or pyrite depletion) compares favourably with those estimated by Postma and Boesen (1990) using a mixing cell model. They also considered variable nitrogen loading as a function of time.

Variation in
redox front
movement rates

Sensitivity studies with the present model showed that the rate of pyrite depletion is almost a linear function of the influx of oxidation potential (i.e. nitrate and oxygen), which again is a linear function of the flow velocity and nitrate and oxygen concentrations and an inverse linear function of the amount of pyrite available. The differences in modelling conditions between this study and that carried out by Postma and Boesen (1990) (e.g. differences in inlet and initial solutions and minerals present) indicates that the nitrate removal processes will occur irrespective of the existence of special chemical environments right at the redox front. Again, this seems to indicate that it is the physical trans-

port processes that have the greatest control on the distribution of nitrate in the aquifer.

5.3.2 Aquifer nitrate contamination

In the previous section it was assumed that nitrate and oxygen were transported directly across the redox front with a representative groundwater velocity of 25 m/year, thus resulting in a reduction capacity removal rate of approximately 40 cm/year. However, the example does not consider the actual three-dimensional groundwater flow pattern at the site. Figure 6, for example, shows that one km away from the water divide, the angle between the velocity vectors at elevations of 20 - 30 m and the almost horizontal layers of pyrite at these depths is very low. This suggests that the mass flux of oxidation potential to these depths will only slowly remove layers of reduction capacity. The calculated rates of redox front movement may therefore not necessarily apply in the real groundwater flow system. In fact, the layers of pyrite may very well effectively prevent any nitrate contamination of the deeper parts of the aquifer. On the other hand, the almost horizontal flow in the aquifer could cause direct discharge of contaminated groundwater to the Rabis Creek.

To investigate the influence of the physical transport processes on the extent of nitrate aquifer contamination the ST3D model coupled with the simple nitrate reaction model (section 4.3.3) has been used.

Flux of nitrate and oxygen to aquifer

The fluxes of oxidation potential (i.e. nitrate and oxygen) to the aquifer have been determined in a manner similar to that proposed by Postma

and Boesen (1990). The amount of oxygen in water percolating to the aquifer is assumed to be fixed at 10 mg/l based on measurements of near-saturation levels in the oxidized zone. The amount of nitrate in water percolating to the aquifer is assumed to increase stepwise from 0 mg/l in 1955 to 80 mg/l in 1970, and remaining here for the rest of the simulation period. The concentrations are yearly averages. These concentration levels are similar to those proposed by Postma and Boesen (1990). The total loading of oxidation potential calculated on the basis of the procedure discussed in section 4.3.3 and the variation in nitrate and oxygen concentrations discussed above are assumed to apply everywhere in the catchment except in the heath and plantations areas where the flux only consists of oxygen. The simulations therefore does not consider the effects of different vegetations and depths to the groundwater table on the flux of oxidation potential to the aquifer.

Location of pyrite

The depths below the groundwater table at which the pyrite reserves have been found are approximately 10 - 15 m, Postma and Boesen (1990). In this study these observations have been assumed to represent the conditions in the whole catchment meaning that there is initially an upper 10 -15 m oxidized zone everywhere and a lower uncontaminated reduced zone. It has been speculated that it is oxygen transport during the 12 - 15000 year period from the last ice age that is responsible for the depletion of the reduction capacity to these depths (Kristiansen et al. (1990)).

Physical and numerical dispersion

The low longitudinal and transverse dispersivities controlling dispersive mixing in the aquifer can not be accurately represented by the ST3D model. This would require a very small mesh in

all directions which can not be accommodated by present day computer facilities. A certain degree of additional numerical dispersion must therefore be accepted. The problem is not as critical in the flow or longitudinal direction as in the vertical direction because we are dealing with a non-point contamination source where the concentration gradients are much smaller in the horizontal than in the vertical direction. At the redox front where the flow streamlines are almost horizontal the numerical dispersion will therefore overestimate the amount of solute dispersed transversely to the flow direction. In addition, the explicit coupling of mass transport and reaction chemistry will cause extra numerical dispersion right at the front.

In order to minimize the amount of dispersion, a finer vertical grid spacing was used in the upper 20 m of the aquifer where most of the mass transport will occur. The dispersivity values determined from tritium simulations at a scale of km's were increased to values of 1 m and 0.1 m for the longitudinal and transverse dispersivities, respectively, in order to represent the larger catchment scale. This scaling up of the dispersivity values is rather arbitrary, especially in the transverse direction where the numerical dispersion (estimated to equal a dispersivity value of about 1 m) will totally obscure the physical dispersion.

Two case runs were considered. In the first case, the oxidation potential was the sum of the contributions from oxygen and nitrate. In the second case, oxygen was neglected. The latter case then has an aquifer initially free of oxidation potential and also zero leaching of oxidation potential below the heath and plantation areas. This case also represents the accelerated movement of

the redox front due to nitrate contamination. It was found that the second case is more illustrative of the hydrogeochemical conditions in the Rabis Creek aquifer, because the extra downward movement of the redox front caused by the presence of oxygen is very small. Only this case will be presented here.

The results are presented as concentration profiles in 1970, 1988 and 2010 at two locations; along the transect of wells, Figure 12, and 1 km south of there, Figure 13. These locations correspond to those shown in Figure 6 for the flow velocity vectors.

Distribution of
nitrate in
aquifer

Both profiles represent a situation where there is zero leaching in the midstream area because of the heath and plantation areas (see Figure 1). Both figures show that in 1970 a plume of nitrate is moving downward from the upstream area to below the plantation or heath area. The plume has just reached the redox front located at approximately 30 m elevation. At the transect of wells this plume is still identifiable in year 2010, while 1 km south of here the plume has already more or less vanished in 1988. This difference in nitrate movement is caused by an upward movement of nitrate-free groundwater at the transect wells (see Figure 6a) mixing with nitrate moving horizontally from the upstream areas.

The plume in 1988 in Figure 12 compares qualitatively to the plume identified by Postma and Boesen (1990). The nitrate levels are lower than those observed. The plume is now right at the redox front in the upstream area. In the mid- to downstream area only small fluxes of nitrate are transported to the redox front. This is also the case in 2010.

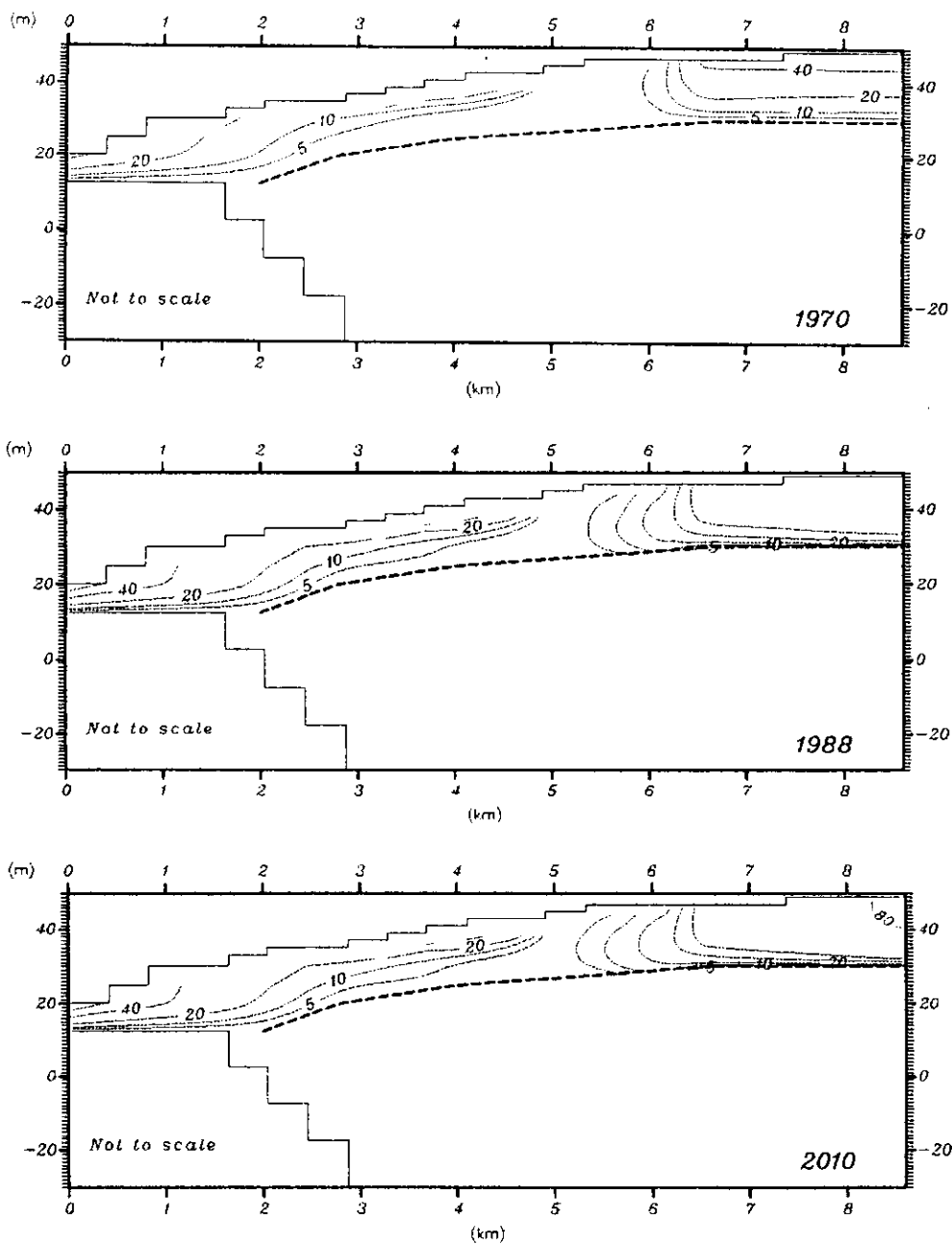


Figure 12. Nitrate concentration contours (mg/l) at the transect of wells in 1970 (top), 1988 (middle) and 2010 (bottom). The redox front is shown as a dashed line.

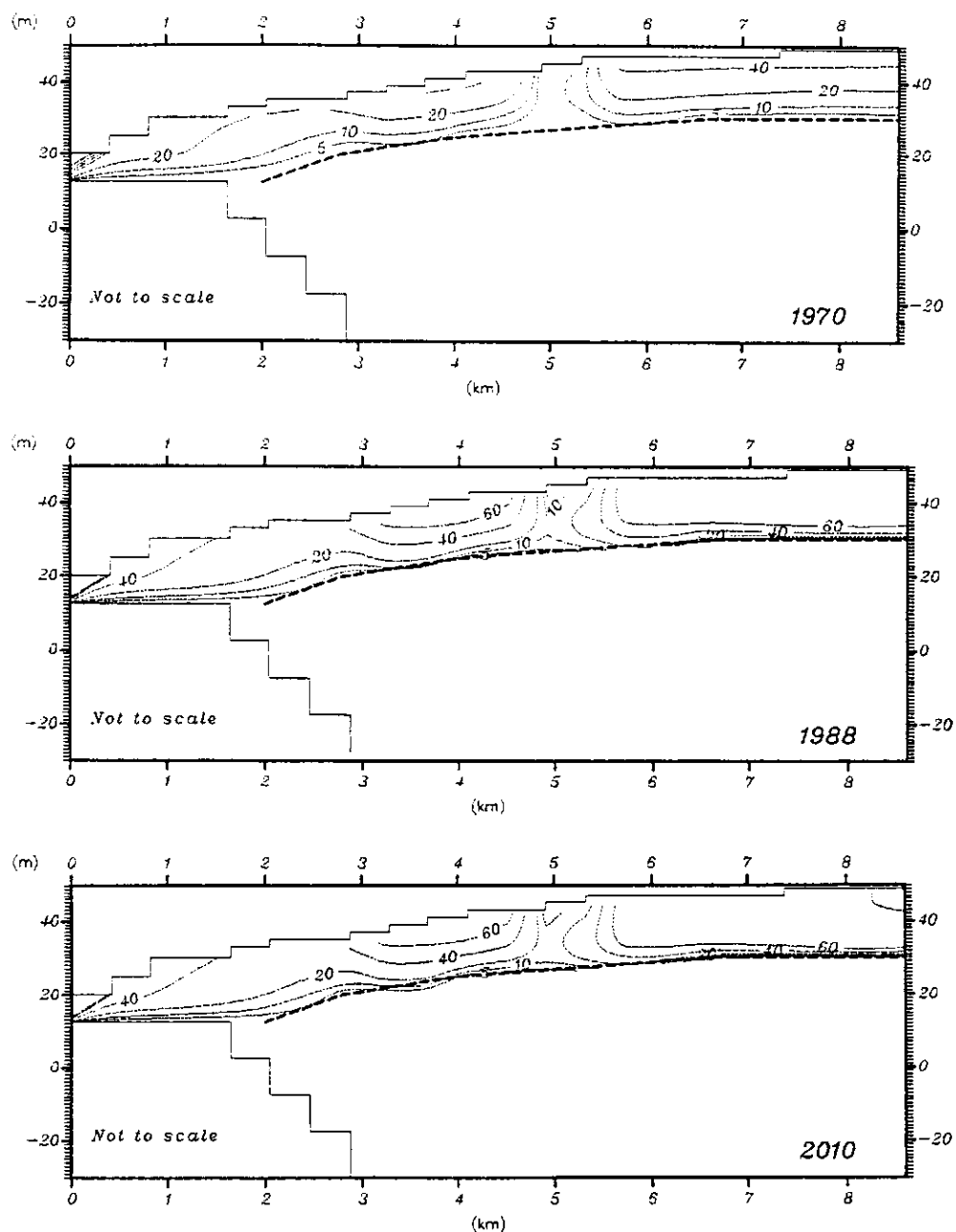


Figure 13. Nitrate concentration contours (mg/l) 1 km south of the transect of wells in, 1970 (top), 1988 (middle) and 2010 (bottom). The redox front is shown as a dashed line.

In Figure 13, however, the plume of nitrate is right at the redox front everywhere in the profile.

Redox front
movement rate

It is evident from Figures 12 and 13 that the redox front practically has no downward movement during the period shown here. The calculated rates are of the orders of cm/year much lower than those predicted, assuming a high mass flux of oxidation potential normal to the redox front, section 5.3.1. The layer of pyrite thus effectively prevent further downward movement of nitrate. These results are of course sensitive to the amounts of pyrite available and also to whether the distribution of pyrite is correct.

Discharge of
nitrate-conta-
minated ground-
water

The simulated nitrate concentration in the creek at Birthesminde is approximately 20 mg NO_3^-/l in 1988, which should be compared to the observed mean annual concentration of approximately 9 mg NO_3^-/l (Hansen, 1990). The difference can be explained by denitrification when nitrate trickles over the adjacent meadows, which is not considered by the model. The reduction in concentration is approximately 50%, which agrees favourably with calculations by Brüsche (Pers.Comm.). These concentration levels and reductions are sensitive to the input function.

Mass balances

Table 3 shows the amount of nitrate discharged to the surface waters and the amount of nitrate removed by denitrification as percentages of the total flux of nitrate into the aquifer at the specified times. Since the nitrate loading function is at an assumed constant level since 1970, a steady state will be achieved. With the conditions given for this case run, approximately 45% of the nitrate leached to the aquifer will reach the surface water system, and approximately 42% will be removed by denitrification over a 95 year

period. The remaining part of the total influx of nitrate is stored in the aquifer. These figures are a result of the groundwater flow pattern and the dispersive mixing in the aquifer. As discussed before, the amount dispersed transversely to the flow direction right at the redox front is overestimated due to numerical dispersion. The calculated percentages are therefore lower and higher for the amount removed and discharged, respectively. With the modelling techniques applied here it is not possible to quantify more precisely the total amount of nitrate that is removed and discharged to the creeks. However, the amount of oxidation potential transported across the front from advection alone was calculated to comprise approximately 80% of the total amount removed by denitrification. This estimate is also affected somewhat by numerical dispersion, but it indicates that vertical flow across the front is the dominant transport mechanism. An estimate of the error introduced by numerical dispersion is then on the order of less than 20%

year	nitrate discharged to creeks	nitrate removed
1960	27%	5%
1965	31%	7%
1970	34%	10%
1977	37%	15%
1988	41%	25%
1999	43%	32%
2010	44%	36%
2021	44%	39%
2050	45%	42%

Table 3. Amount of nitrate discharged to the creeks (Karup and Rabis) and amount of nitrate removed as percentages of total flux of nitrate to the aquifer.

and probably closer to 10%. The amount of nitrate removed should then be decreased by 10% and is in the year 2050 then only approximately 37%, while the discharge of nitrate to the creeks is closer to 50%. Notice that the increase in nitrate removal is highest in the mid 70's. This corresponds to the time when most of the plume has reached the redox front.

6. Conclusions

Transport and removal of nitrate in the Rabis Creek aquifer have been modelled in a three stage approach. In the first two stages, the physical processes responsible for nitrate transport were investigated, while in the third stage, simple nitrate removal processes were assumed to represent denitrification processes that occur in the aquifer.

Groundwater flow	The groundwater flow pattern is almost horizontal in the aquifer but with significant downward or upward flow at the water divide and Rabis Creek only. The upward flow close to Rabis Creek comes from the deeper parts of the aquifer.
Tritium transport	Tritium simulations show that the longitudinal and transverse dispersivity values that control the amount of dispersive mixing in the aquifer are very low. However, these can result in significant mass dispersion in the aquifer over the long time scales considered. Furthermore, the sharp nitrate and oxygen profiles observed by Postma and Boesen (1990) are most likely due to fast reaction chemistry and not to low dispersive mixing. The results also show that the mass flux of nitrate and oxygen due to dispersion transversely to the almost horizontal streamlines at the redox front will be small.

Reactive nitrate
transport

It has been demonstrated that given a high flux of oxidation potential to the redox front this front separating the oxidized and reduced zones will move at a rate that is proportional to the amount of mass flux of oxidation potential, which again is a function of the groundwater velocity and the nitrate and oxygen concentrations. A typical rate is 40 cm/year. The rate of redox front movement is probably only slightly affected by variations in the groundwater composition of other constituents. This has not been verified directly, but is based on differences in the model studies by Postma and Boesen (1990) and Engesgaard and Kipp (1990).

When it is attempted to take the real three-dimensional groundwater flow pattern into account, the rate of redox front movement in the vertical direction decreases significantly. The rate is more on the order of cm's/year in the vertical direction. This is caused by a low flux of oxidation potential to the redox front due to nearly horizontal flow at the zone of reaction. The layer of reduction capacity will thus protect the deeper parts of the aquifer.

The composition of the groundwater base flow to Rabis Creek is a mix between nitrate-free groundwater from the deeper parts of the aquifer and nitrate-contaminated groundwater from the upstream areas. The difference in simulated and observed nitrate concentrations in the creek indicates that the denitrification processes that take place when nitrate trickles over the adjacent meadows can account for up to a 50% reduction in nitrate concentration.

With the modelling techniques applied in this study, the simulations indicate that given the conditions specified for the case runs a little more than one-third of the total amount of

nitrate leached to the aquifer will be removed, while close to one-half will be discharged to the creek on a long term basis (year 2050). In 1988 less than one-fourth of the total amount leached to the aquifer had been removed.

The application of several numerical models have been the basis for the simulation results and conclusions presented in this report. The results represent the best attempt to date of describing reactive movement of nitrate in the Rabis Creek aquifer. The results and conclusions should be viewed in the light of the assumptions and simplifications that were necessary to complete this model study.

Since the groundwater flow pattern in the Rabis Creek aquifer has a major influence on the results, the conclusions presented here will not necessarily apply elsewhere.

7. Acknowledgements

This work was in many aspects a team effort between the authors and research hydrologist Kenneth Kipp, U.S. Geological Survey, USA, which is gratefully acknowledged.

8. References

- Andersen, L.J. and T. Sevel (1974). Six years environmental tritium profiles in the unsaturated and saturated zones, Grønhøj, Denmark, in "Isotope techniques in groundwater hydrology 1974", vol.1, IAEA-SM-182/1.
- Brüsch, W. and I. Bendix (1987). Grundvandskemi i udvalgte engarealer, -grundvandskemi og -strømning i og ved Rabis bæk's øvre løb, Karup Hedeslette, Marginaljorder og Miljøinteresser, Miljøministeriets projektundersøgelser 1986, Teknikerrapport nr. 20. (In Danish)
- Egboka, B.C.E., J.A. Cherry, R.N. Farvolden and E.O. Frind (1983). Migration of contaminants in groundwater at a landfill: A case study. 3. Tritium as an indicator of dispersion and recharge. Journal of Hydrology, 63, pp. 51-80.
- Engesgaard, P. and K.H. Jensen (1990). Drainage flow modelling - Syv Field Site, NPo-forskning fra Miljøstyrelsen B14.
- Engesgaard, P. and K. Kipp (1990). A geochemical model for redox-controlled movement of mineral fronts in ground-water flow systems: A case of nitrate removal by oxidation of pyrite. (To be submitted for publication).
- Engesgaard, P. (1988). Two-dimensional areal and profile groundwater modelling. Nordisk Hydrologisk konferens 1988, Nordisk NHP-rapport nr. 22, Del 2.

- Frind, E.O., W.H.M Duynisveld, O. Strebel, and J. Boettcher (1989). Simulation of nitrate and sulfate transport and transformation in the Fuhrberger Feld aquifer, Hannover, Germany. In Proceedings International Symposium on Contaminant Transport in Groundwater, Germany, April 1989, pp. 97-104, Kobus and Könzelbach (Eds.), Balkema, Rotterdam.
- Gvirtzmann, H., M. Magaritz, H. Kanfi and I. Carmi (1988). Matrix and fissure water movement through unsaturated calcareous sandstone, Transport in Porous Media, 3, pp. 343-356.
- Hansen, B. (1990). Afstrømning og transport til Rabis og Syv bæk. NPo-forskning fra Miljøstyrelsen B9. (In Danish).
- Herweijer, J.C., G.A. Van Luijn and C.A.J. Appelo (1985). Calibration of a mass transport model using environmental tritium, Journal of Hydrology, 78, pp. 1-17.
- Jensen, K.H. (1983). Simulation of water flow in the unsaturated zone including the root zone. Institute of Hydrodynamics and Hydraulic Engineering. Technical University of Denmark, Series Paper no. 33, 259 pp.
- Keidser, A., P. Engesgaard and D. Rosbjerg (1990). Application of inverse modelling in the Rabis Creek catchment. (To be printed in Progress Report, Inst. Hydrodyn. and Hydraulic Eng.).
- Kinzelbach, W. and W. Schäfer (1989). Coupling of chemistry and transport. Groundwater Management: Quantity and Quality, proceedings of the Benidorm Symposium, October 1989, IAHS publication 188, pp. 237-259.

- Kipp, Jr., K.L., HST3D (1987). A computer code for simulation of heat and solute transport in three-dimensional groundwater flow systems, U.S. Geological Survey, Water Resources Investigations Report, 86 - 4095.
- Konikow, L.F. and J.D. Bredehoeft (1978). Computer model of two-dimensional solute transport and dispersion in groundwater, Techniques of Water Resources Investigations of the United States Geological Survey, Chapter C2.
- Kristiansen, H., W. Brusch and P. Gravesen (1990). Transport og omsætning af kvælstof og fosfor i Rabis baks opland. NPo-forskning fra Miljøstyrelsen B17. (In Danish).
- Miljøstyrelsen (1983). Karup Å undersøgelsen, Miljø-projekter 51, Environmental Protection Agency of Denmark. (In Danish).
- Olesen, J. (1990). Klimastationer i NPo-værkstedsområder, NPo-project B17, Environmental Protection Agency of Denmark. (In Danish).
- Overgaard, K. (1984). Trends in nitrate pollution of groundwater in Denmark. Nordic Hydrology, vol. 15, pp. 117-184.
- Parker, J.C. and Th. van Genuchten (1984). Determining Transport Parameters from Laboratory and Field Tracer Experiments, Bulletin 84-3, Virginia Agricultural Experiment Station.
- Parkhurst, D.L., D.C. Thorstenson, and L.N. Plummer (1980). PHREEQE - A computer program for geochemical calculations, U.S. Geological Survey Water Resources Investigations Report.

- Postma, D. and C. Boesen (1990). Processes of nitrate reduction in a sandy aquifer, NPO-forskning fra Miljøstyrelsen, B8.
- Rifai, H.S. and P.B. Dedić (1990). Comparisons of biodegradation kinetics with an instantaneous reaction model for groundwater, Water Resources Research, Vol 26(4), pp. 637-645.
- Robertson, W.D. and J.A. Cherry (1989). Tritium as an indicator of recharge and dispersion in a groundwater system in central Ontario. Water Resources Research, Vol. 25(6), pp. 1097-1109.
- Sevel, T., N. Kelstrup and K. Binzer (1981). Ned-sivning. Dansk komite for hydrologi, Rapport nr. Suså H6.
- Storm, B. (1990). Regional model for næringssalt-transport og omsætning, NPO-project B15. Environmental Protection Agency of Denmark. (In Danish).

Registreringsblad

Udgiver: Miljøstyrelsen, Strandgade 29, 1401 København K.

Serietitel, nr.: NPo-forskning fra Miljøstyrelsen, B13

Udgivelsesår: 1990

Titel:

Flow and Transport Modelling - Rabis Field Site

Undertitel:

Forfatter(e):

Engesgaard, Peter; Jensen, Karsten Høgh

Udførende institution(er):

Danmarks Tekniske Højskole. Institut for Strømningsmekanik og Vandbygning

Resumé:

3-dimensionale simuleringer af nitrattransport og -omsætning i grundvandsmagasinet ved Rabis bæk viser, at forureningsområdet hovedsagelig er kontrolleret af grundvandsbevægelsen.

Afstrømningen til Rabis bæk består af både dybereliggende nitrattæt og overfladenært nitrattæt grundvand. Over en 100-års periode er der simuleret, at ca. 1/3 og 1/2 af den totalmængde nitrat, der tilføres magasinet, fjernes ved denitrifikation henholdsvis afstrømmer til Rabis bæk og Karup å.

Emneord:

grundvand; afstrømning; udvaskning; transport; denitrifikation; hydrologiske modeller; akvifer; nitrogen CAS 7727-37-9

ISBN: 87-503-8806-1

ISSN:

Pris: 70,- kr. (inkl. 22% moms)

Format: A5

Sideantal: 64 s.

Md./år for redaktionens afslutning: november 1990

Oplag: 550

Andre oplysninger:

Rapport fra koordinationsgruppe B for grundvand

Tryk: Notex-Grafisk Service Center as

Data Sheet

Publisher: Ministry of the Environment,
National Agency of Environmental Protection,
Strandgade 29, DK-1401 Copenhagen K.

Serial title and no.: NPo-forskning fra Miljøstyrelsen, B13

Year of publication: 1990

Title:

Flow and Transport Modelling - Rabis Field Site

Subtitle:

Author(s):

Engesgaard, Peter; Jensen, Karsten Høgh

Performing organization(s):

Institute of Hydrodynamics and Hydraulic Engineering (ISVA),
Technical University of Denmark, Building 115, DK-2800 Lyngby

Abstract:

3-dimensional simulations of reactive nitrate transport in the Rabis Creek aquifer show that the extent of nitrate contamination is groundwater flow controlled. The discharge to Rabis Creek is a mix between nitrate-free groundwater from the deeper parts of the aquifer and upper nitrate-contaminated groundwater. A long-term simulation shows that approximately 1/3 and 1/2 of the total flux of nitrate to the aquifer is removed by denitrification and discharged to the creek, respectively.

Terms:

groundwater; surface runoff; leaching; transport; denitrification;
hydrological models; aquifer

ISBN: 87-503-8806-1

ISSN:

Price (incl. 22% VAT): 70,- Dkr.

Format: AS5

Number of pages: 64 p

Edition enclosed (month/year): November 1990

Circulation: 550

Supplementary notes:

Report from coordination group B for groundwater

Printed by: Notex-Grafisk Service Center as. Denmark

NPo-forskning fra Miljøstyrelsen

Rapporter fra koordinationsgruppe B for grundvand

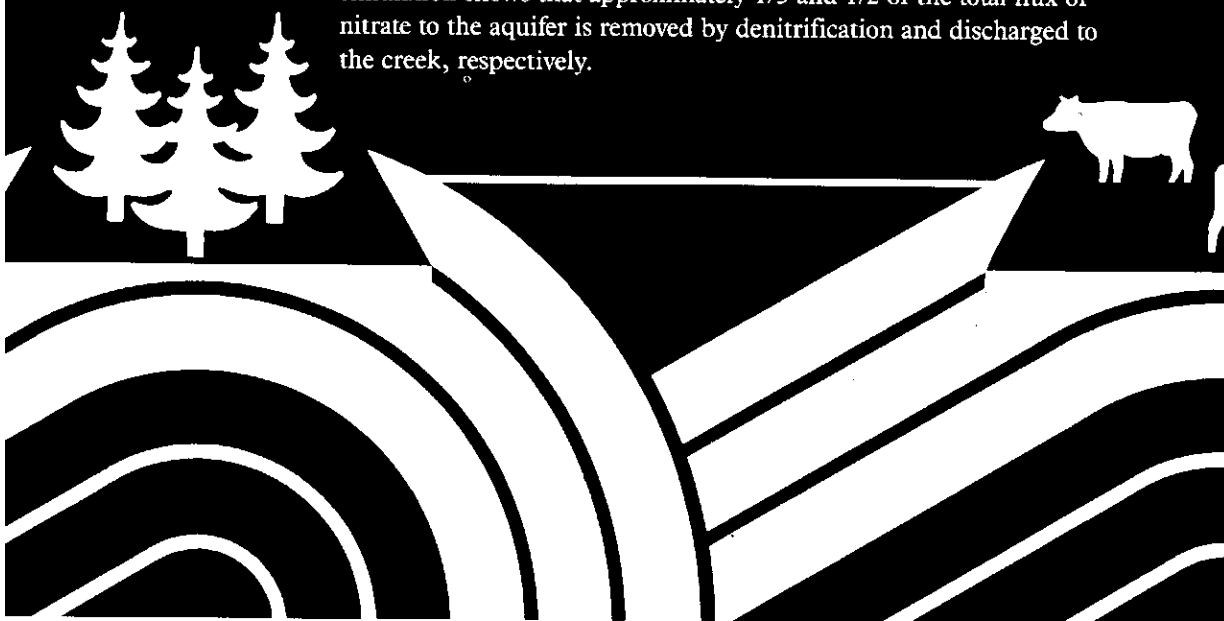
- Nr. B1 : Kemisk nitratreduktion med jern(II)forbindelser
- Nr. B2 : Nitratreduktion i moræner
- Nr. B3 : Nitratreduktion og organisk stof i grundvandsmagasiner
- Nr. B4 : Nitrat og fosfat i grundvand/drikkevand fra områder i Danmark
- Nr. B5 : Transport og omsætning af N og P i Rabis Bæks opland
- Nr. B6 : Transport og omsætning af N og P i Langvad Ås opland - 1
- Nr. B7 : Transport og omsætning af N og P i Langvad Ås opland - 2
- Nr. B8 : Nitratreduktionsprocesser i Rabis hedesletteaquifer
- Nr. B9 : Afstrømning og transport til Rabis og Syv Bæk
- Nr. B10 : Geokemiske processer i et grundvandsmagasin
- Nr. B11 : Grundvandsbelastning fra to landbrug på sandjord
- Nr. B12 : Fluktuationer i grundvandets nitratinhold
- Nr. B13 : Flow and Transport Modelling - Rabis Field Site
- Nr. B14 : Drainage Flow Modelling - Syv Field Site
- Nr. B15 : Regional model for næringssalttransport og -omsætning
- Nr. B16 : Kortlægning af potentialet for nitratreduktion
- Nr. B17 : Klimastationer i NPo-værkstedsområder
- Nr. B18 : Grundvandsmoniteringsnet i Danmark
- Nr. B19 : Field Investigations of Preferential Flow Behaviour

Nr. B8 er tidligere annonceret med titlen:

Processes of nitrate reduction in a sandy aquifer

Flow and Transport Modelling - Rabis Field Site

3-dimensional simulations of reactive nitrate transport in the Rabis Creek aquifer show that the extent of nitrate contamination is groundwater flow controlled. The discharge to Rabis Creek is a mix between nitrate-free groundwater from the deeper parts of the aquifer and upper nitrate-contaminated groundwater. A long-term simulation shows that approximately 1/3 and 1/2 of the total flux of nitrate to the aquifer is removed by denitrification and discharged to the creek, respectively.



Miljøministeriet **Miljøstyrelsen**

Strandgade 29, 1401 København K, tlf. 31 57 83 10

Pris kr. 70.- inkl. 22% moms

ISBN nr. 87-503-8806-1